

NASA/CR-1998-207797

N-31-261
119154

FINAL REPORT

**LOW COST CRYOCOOLERS FOR HIGH TEMPERATURE SUPERCONDUCTOR
COMMUNICATION FILTERS**

NASA AITP COOPERATIVE AGREEMENT NCC5-117

APRIL 1998

LOCKHEED MARTIN/ADVANCED TECHNOLOGY CENTER

SUPERCONDUCTOR TECHNOLOGIES, INC.

NATIONAL INSTITUTE OF STANDARDS AND TECHNOLOGY

NASA GODDARD SPACE FLIGHT CENTER

FOREWORD

This final report describes the work performed by a consortium of Industry and Government to develop low cost cryocoolers. The specific application was for low cost commercial based high temperature superconductor communication filters.

This program was initiated in January 1995 and resulted in the successful demonstration of an HTS filter dewar cooled by a low cost pulse tube cryocooler. Further development of this cryocooler technology is proceeding through various contracts underway and proposed at this time.

The members of the consortium and their contributions are summarized below.

Lockheed Martin Advanced Technology Division (LMATC) led the consortium and was responsible for the development of the flexure bearing compressor and the pulse tube. The final integration and testing of the cryocooler—dewar assembly was performed at LMATC. The leader of this team was T. Nast.

Superconductor Technology, Inc. (STI) had the responsibility to develop the gas bearing compressor to be integrated with the pulse

tube. They also were responsible for the development of the HTS filter package which was integrated with the pulse tube cryocooler, and the specifications for the cryocooler system. They provided help in pulse tube modeling through their consultant David Gedeon who contributed much valuable analysis and guidance. The leader of this effort was initially Tim James and later Vince Luong.

The National Institute of Standards and Technology provided help in the pulse tube modeling and design and provided the design for the first of three pulse tube designs developed under this program. Dr. Ray Radebaugh led this effort.

NASA Goddard Space Flight Center provided support in meetings and offered guidance in the development of the cryocooler. Dr. Steve Castles supported many of the meetings and provided valuable insight into the pulse tube development.

Vince Bly of NASA GSFC was the technical monitor of this program, and although his attendance at meetings was limited, provided perceptive insight into some of the development areas.

TABLE OF CONTENTS

Section	Page
1.0 INTRODUCTION.....	1-1
2.0 PROGRAM GOALS AND REQUIREMENTS.....	2-1
3.0 HARDWARE DEVELOPMENT	3-1
3.1 FLEXURE BEARING COMPRESSOR	3-1
3.2 GAS BEARING COMPRESSOR	3-4
3.3 PULSE TUBE COLDHEAD.....	3-5
3.3.1 Initial Design - In-line Pulse Tube	3-5
3.3.2 Fabrication of the In-line Pulse Tube	3-6
3.3.3 Design and Fabrication of the Concentric Pulse Tube, Filter Dewar Integration.....	3-8
3.4 ELECTRONIC CONTROLLER	3-8
4.0 TEST DATA	4-1
4.1 TEST APPARATUS	4-1
4.2 TEST RESULTS	4-3
4.2.1 Flexure Bearing Compressor In-line Pulse Tube Test	4-3
4.2.2 Gas Bearing Compressor In-line Pulse Tube Test	4-4
4.2.3 Flexure Bearing Compressor Concentric Pulse Tube Tests.....	4-4
4.2.4 Concentric Pulse Tube - Filter Package System Test	4-6
4.2.5 Etched Foil Regenerator Development	4-7
4.2.6 DC Flow Investigation	4-10
5.0 SYSTEM COST PROJECTIONS.....	5-1
5.1 FLEE BEARING COMPRESSOR	5-1
5.2 GAS BEARING COMPRESSOR	5-2
5.3 SYSTEM COST STUDIES	5-3
6.0 BUSINESS AND COMMERCIALIZATION PLAN	6-1
7.0 NEW TECHNOLOGIES DEVELOPED (PATENTABLE).....	7-1
7.1 LINEAR MOTOR	7-1
7.2 FLEXURE BEARING ALIGNMENT	7-1
7.3 PISTON/CYLINDER ALIGNMENT	7-1
7.4 POSITION SENSOR.....	7-2
8.0 ADVANCED DERIVATIVES UNDERWAY FROM THIS TECHNOLOGY.....	8-1
8.1 DARPA PROGRAM FOR HIGH TEMPERATURE SATELLITE COMMUNICATION SYSTEMS	8-1
8.2 NASA/GSFC MINIATURE PULSE TUBE CRYOCOOLER.....	8- 3
9.0 SUMMARY AND CONCLUSIONS.....	9-1

LIST OF ILLUSTRATIONS

Figure		Page
2-1	Principal requirements for pulse tube cryocooler	2-1
3-1	Approach for achieving low cost design	3-1
3-2	Compressor with internal parts	3-1
3-3	Motor housing assembly	3-2
3-4	Motor housing	3-2
3-5	Suspension springs	3-3
3-6	Cylinder support	3-3
3-7	Gas bearing compressor specifications	3-4
3-8	Gas bearing compressor configuration	3-5
3-9	Linear motor design for gas bearing compressor	3-5
3-10	Original integration design with in-line pulse tube	3-6
3-11	Design parameters of the pulse tube coldhead	3-7
3-12	DC flow control	3-8
3-13	Layout of flexure bearing pulse tube integrated with HTS filter dewar	3-9
3-14	Interface details between coaxial pulse tube and dewar	3-9
3-15	Specifications for electronic controller for pulse tube cryocooler	3-10
3-16	Electronic controller to drive compressor	3-10
4-1	Text matrix for concentric pulse tube	4-1
4-2	Text apparatus for in-line pulse tube	4-2
4-3	Load lines for in-line pulse tube	4-3
4-4	Specific power for in-line pulse tube	4-4
4-5	Performance summary of in-line pulse tube	4-4
4-6	Power balance of Compressor B	4-4
4-7	STI compressor/pulse tube cooling tests	4-5
4-8	Comparative testing on concentric and in-line configuration (second design)	4-5
4-9	Flexure Bearing—concentric pulse tube integrated with STI HTS filter package ..	4-7
4-10	Flexure Bearing—concentric pulse tube integrated with STI HTS filter package ..	4-8
4-11	Flexure Bearing—concentric pulse tube integrated with STI HTS filter package ..	4-8
4-12	Flexure Bearing—concentric pulse tube integrated with STI HTS filter package ..	4-9
4-13	Measured RF response for HTS filter dewar—pulse tube cryocooler tests	4-9
4-14	Summary of tests comparing the etched foil generator with screens	4-10
4-15	Regenerator/pulse tube temperature profile	4-11
4-16	Cooling power and the accompanying regenerator and pulse tube midpoint temperatures	4-12
5-1	Composite prices by component	5-1
5-2	Composite prices comparing manufacturing approaches	5-2
5-3	Compressor cost summary for STI gas bearing compressor system	5-3
5-4	Current commercial cryocooler cost estimate	5-3
6-1	Markets and Products—Commercial Wireless Market (cellular)	6-1
6-2	Markets and Products—Commercial Wireless Market (cellular)	6-1
6-3	Markets and Products—Military Wireless	6-1
6-4	STI's Stirling cooler development snapshot	6-2
6-5	STI's interest in pulse-tube technology	6-2
6-6	Required program to insert pulse tube into products	6-2

LIST OF ILLUSTRATIONS (cont.)

Figure		Page
6-7	Proposed cryocooler development program	6-3
8-1	Utilization of head to head compressors for a low pulse tube	8-1
8-2	Load line of pulse tube with head to head low cost compressors	8-2
8-3	Specific compressor power for pulse tube with head to head low cost compressors	8-3
8-4	45 Hz coldhead performance	8-3
9-1	Summary of major accomplishments of the NASA/AITP program	9-1

1.0 INTRODUCTION

This is the final report for a program to develop low cost cryocooler technology for High Temperature Superconductor Communication Filters. This work was performed under a NASA Aerospace Technology Program (AITP) Cooperative Agreement No. NCC5-117. The program started in February 1995 and was completed in April, 1998.

A consortium of federal and industry partners has successfully developed cryocooler technology for low cost commercial applications directed at ultraselective radio-frequency filters for communication systems such as cellular phones. The consortium was led by the Advanced Technology Division of Lockheed Martin Missiles & Space in partnership with Superconductor Technology, Inc. (STI), a small business in Santa Barbara, California, the National Institute of Standards and Technology (NIST) in Boulder Colorado, and NASA's Goddard Space Flight Center in Greenbelt, Maryland.

One of the keys to the commercial success of this technology is the cost and reliability of the cryocooler. In order to offer a viable technology, the cryocoolers must operate for over 40,000 hours with very high reliability, and be available at low cost.

The principle approach for this program was to develop efficient pulse tubes to be utilized with the flexure bearing compressor, developed by LM and the gas bearing compressor, under development at STI. Both of these approaches have demonstrated long life capability and have no systematic wear out characteristics. In theory either compressor technology can provide unlimited lifetimes, since there are no life limiting mechanisms.

The flexure bearing technology was originally developed by Oxford University and this technology propagated to various companies in Great Britain and the United States. At LM

we have been developing this technology since 1987 for utilization on long life space missions, and have established demonstrations of long life capability (in excess of 3 years). In this approach the moving parts are supported by flexures which operate below their infinite fatigue life and the gas seal is achieved by a clearance seal which eliminates rubbing or wear but minimizes the gas leakage from the compression space. It is the alignment of this clearance seal which is one of the major cost drivers. Various companies have demonstrated run times as long as 6 years, without failure. While this technology has matured and demonstrated the required reliability and lifetime, the cost of present space borne systems is prohibitive for commercial applications. One of the major goals in this program was to redesign the compressor in such a way that we retain the unlimited lifetime of the technology at a greatly reduced cost. As will be described, this objective was achieved with a novel moving magnet linear motor in combination with self aligning features of the required clearance seal systems.

The alternative technology under development at STI also eliminates any rubbing or wear by a clearance gap but achieves the centering of the piston in the clearance gap by pressurized working gas. The technique for pressurizing this space is unique. Compressors of this type have also shown long run times without wear, although the number of tests and duration of run times is not as mature as for the flexure bearing systems.

In the past, these compressors have been utilized to drive a displacer in the Stirling cycle system. The displacer in the Stirling system is driven by a motor or pneumatic effects from the pressurizing gas and requires techniques for alignment or centering of the moving parts to avoid rubbing or wear. These techniques are similar to those utilized for the compressor.

and substantially add to the cost and drive down the reliability.

In this program, we eliminated the displacer and replaced it by a new device referred to as a pulse tube. In the pulse tube, the thermodynamic principles are similar but certain phase shifting mechanisms which produce the cooling are achieved in a passive manner, without moving parts. This approach greatly reduces the cost of the system and improves reliability. There are other benefits, such as the

lack of vibration from the pulse tube cold head. While the pulse tube has many obvious benefits over the Stirling, the thermodynamic efficiency has been substantially lower for the pulse tube except in a few notable cases.

Several investigators, including LM have developed pulse tube systems which have equal or better power efficiency than the Stirling, and this has greatly stimulated interest in the pulse tube systems.

2.0 PROGRAM GOALS AND REQUIREMENTS.

At the onset of this program we established the following principle goals:

Lifetime: Greater than 40,000 hours (4.56 years)

Cooling Capability: 4 W at 80 K

Cost: \$1000 each in Production Quantities of 1,000 units per year

Two major requirements of the program were to integrate the selected pulse tube cryocooler(s) with an HTS filter package produced by STI and demonstrate all up system performance. Additionally one of the requirements was to produce a business/commercialization plan for further development.

During the program these requirements were further defined and refined and resulted in the more specific cryocooler goals summarized in *Figure 2-1*.

Abstracted From Requirements Document	
Required Cooling	2.5 W @ 74 K $T_{inlet\ air} = 55\ C$
Cooling Goal	3.0 W @ 74 K $T_{inlet\ air} = 55\ C$
Power Goals	<85 W $T_{inlet\ air} = 25\ C$ <185 W $T_{inlet\ air} = 55\ C$
Operating Orientation	Any
Design Structural Loads	
Operating	Seismic
Non-Operating	Transportation
Weight	<3 Kg

Figure 2-1. Principal Requirements for Pulse Tube Cryocooler

3.0 HARDWARE DEVELOPMENT

3.1 FLEXURE COMPRESSOR

Because one of the principle thrusts of the program was to reduce production costs major emphasis was placed on low cost design. The basis approach to achieve this is summarized in *Figure 3-1*.

- | |
|---|
| <ul style="list-style-type: none"> • Elimination of precision parts and moving parts in cold head by replacing displacer with pulse tube |
| <ul style="list-style-type: none"> • Reducing compressor cost while maintaining long life characteristics of flexure bearing/clearance seal <ul style="list-style-type: none"> - Moving magnet motor reduces parts and electrical feedthroughs - Modular assembly - External sensors reduce parts count eliminates electrical feedthroughs - Self aligning flexure bearing system |
| <ul style="list-style-type: none"> • These features reduce parts count and assembly time |

Figure 3-1. Approach for achieving low cost design

This section describes the development of the hardware. Two compressor approaches were developed. The flexure bearing/clearance seal compressor was developed at LMATC and the gas bearing approach was developed at STI.

The goal of the LCC compressor design was to maintain the long-life and reliability advantages of classic space-borne systems while dramatically lowering manufacturing costs.

This was accomplished by using the proven clearance seal and flexure suspension piston system of the space-type compressors, but changing to a moving magnet motor and a redesigned housing. In addition, features were added to allow automation of the critical piston/cylinder alignment procedure, thus reducing assembly time.

This moving magnet motor architecture enables several design features which provide significant cost and performance advantages over the moving-coil approach.

The compressor is combined with an attached passive balancer and forced-air external cooling to be readily adaptable to ground-based installations.

Fewer Parts

The moving-magnet design lowers costs while improving reliability by reducing the number of parts. Multiple parts were combined into single parts to perform multiple functions.

Figure 3-2 demonstrates the simplicity of a moving-magnet compressor design by showing the low cost compressor with all its internal parts. Eliminated are flex leads,

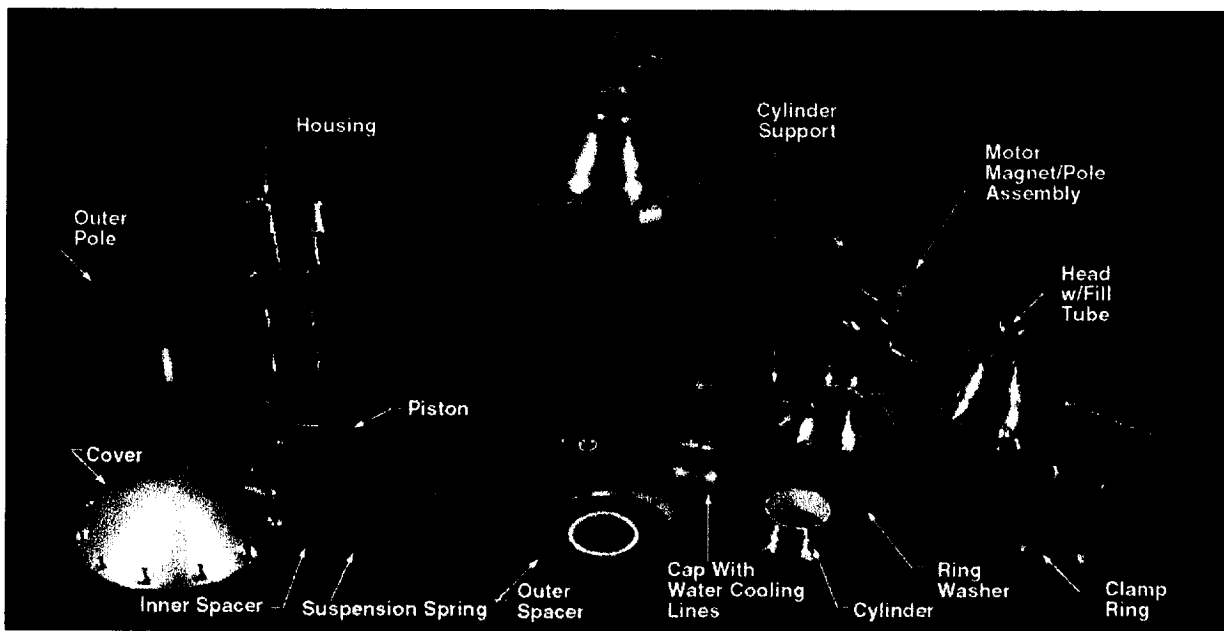


Figure 3-2. Compressor With Internal Parts. The compressor reduces cost with decreased parts count

connectors, insulators, terminals, and coil carrier.

The single-piece motor housing integrates both of the suspension spring mounting bores into the pressure casing and includes the dual recesses that accommodate the external coils and outer magnetic pole pieces. Due to this single-piece housing, there are only two joints in the pressure casing, both designed for welding to ensure long-term sealing.

Moving Magnet Motor

Moving-magnet motors, while inherently simpler and more reliable than moving-coil types, typically have increased moving mass, which in this case is desirable for achieving the optimum frequency.

The moving-magnet motor architecture removes the coil and its possible contaminants from the working fluid, as shown in *Figure 3-3*, simplifying system bake-out and improving reliability. It also eliminates the need for flexing coil leads. This means that no electrical connections are required through the pressure wall.

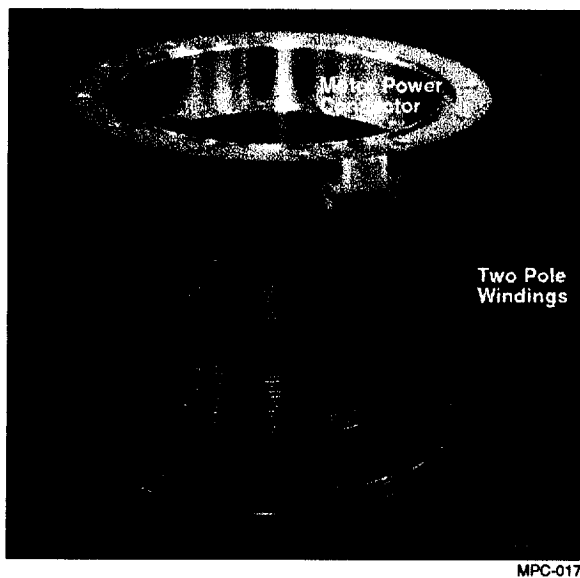


Figure 3-3. Motor Housing Assembly. External winding (outer pole removed) simplifies motor design, reducing cost and increasing reliability

The magnetic position sensor used with this design mounts outside the housing, as shown in *Figure 3-4*, and senses motion of the motor's moving magnets. This design eliminates extra parts on the moving assembly and the need for electrical connections through the pressure wall.

The moving inner pole piece, unique to this design, has several advantages. It eliminates the close-tolerance fit required of fixed inner poles and again reduces parts count. In addition, since the motor's magnetic field is not moving relative to this pole, there are no induced eddy-current losses. This improves overall motor efficiency.

Self-Centering Suspension

The first step of the precision alignment required in clearance-seal type compressors is centering the piston shaft to achieve precise and stable linear motion. This is accomplished with the unique suspension springs shown in *Figure 3-5*. They include a built-in self centering feature using a tri-beam mechanism that flexes to mate to the shaft with a controlled interference fit at three points. A similar arrangement is used on the outer diameter to mate to the housing bore. This eliminates the need for additional centering proce-

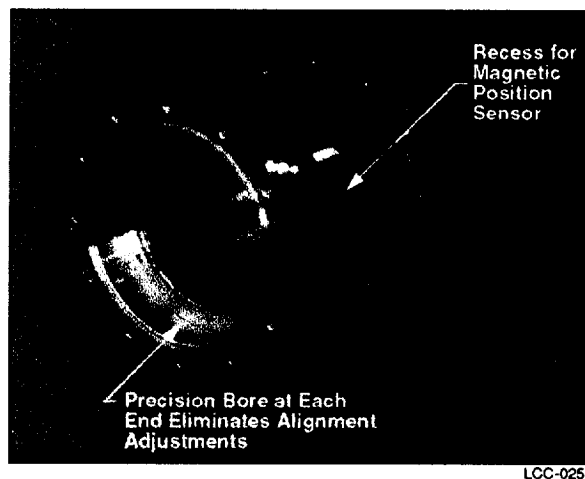


Figure 3-4. Motor Housing. One piece design eliminates need for alignment

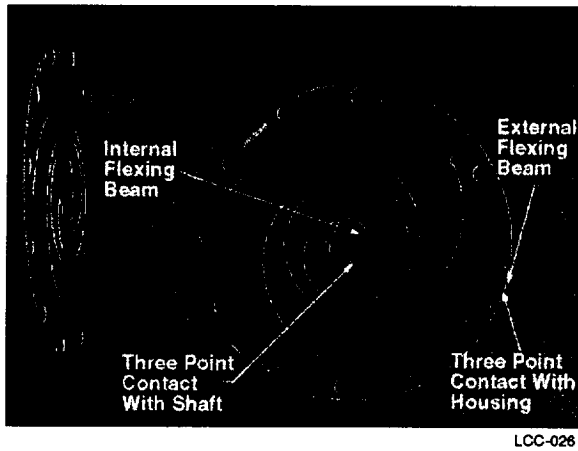


Figure 3-5. Suspension Springs. Self-aligning springs reduce assembly time and cost, and improve repeatability

dures during assembly and ensures long-term stability since centering is not affected by fastener torque.

Since the suspension springs are produced by a chemical milling process and the tri-beam features are part of the photo-etch mask, no additional costs are associated with these mechanisms.

A mating tri-lobe piston shaft simplifies the motor assembly procedure by allowing the magnet assembly and springs to be installed into the housing separately without special fixturing. The shaft is inserted through these parts with the flats aligned to the springs and then simply rotated 60° to engage the tri-beams of the springs, centering itself as well as the magnet assembly.

The one-piece housing shown in Figure 3-3 includes precision bores on both ends which accept these self-centering flexures. This eliminates the need for end-to-end alignment during assembly and results in permanent precise linear motion of the piston.

Automated Alignment

The final step of the alignment is to center the clearance seal cylinder on the piston, matching both its tilt and its position. This is accomplished with a custom-designed auto-

mated alignment facility combined with a new tilt adjustment mechanism.

The cylinder support shown in Figure 3-6 has a built-in screw-type adjustment mechanism which allows for controlled, precise adjustment of tilt in both axes during the alignment procedure. This mechanism is integrated into the design of the cylinder support without adding any extra parts.

The automated compressor alignment facility consists of a special fixture using micropositioners coupled with force and position feedback transducers, all of which can be tied together under computer control. It achieves both the final tilt and the centering of the cylinder relative to the piston using a step-by-step procedure with measured results. Trial and error procedures are eliminated.

Long-Term Dimensional Stability

The simplified motor design combined with component material selection results in improved stability, increasing life and reliability.

All parts involved in the critical core module (housing, springs, shaft, piston) are made of stainless steel. Differential thermal expansion is thus eliminated as a possible cause of alignment drift.

The critically aligned piston/cylinder parts are isolated from the cylinder head (front

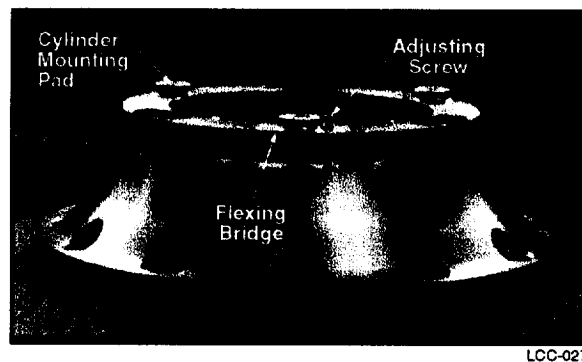


Figure 3-6. Cylinder Support. This support with integrated tilt adjusting mechanism is part of the automated alignment system

housing) to prevent distortion during compressor installation and mounting.

Built-in resilient hard stops at both ends of travel protect critical parts from possible damage during overstroking.

Passive Vibration Balancer

The cryocooler system is configured with a passive balancer for vibration cancellation of the compressor moving parts. This allows the cooler system to operate with the inherent efficiencies of a single compressor while still achieving first-order vibration cancellation.

Advantages Over Front-to-Front Configurations

The balancer offers the following advantages:

- Considerable weight savings compared to dual compressor configurations because of the simplified structure of the balancer
- No requirement for a sealed high-pressure environment
- No requirement for ultra-precision mechanical components due to the absence of the clearance seals

Balancer Suspension

The spring suspension for the compressor balancer mass uses a spiral diaphragm flexure similar to the compressor. This ensures that the fundamental motion of the mass and any secondary motions of the suspensions system (including the slight axial rotations inherent in spiral spring suspensions) are exactly duplicated, in reverse, in the balancer.

To match the operating frequency of the compressor, the stiffness of the suspension must be increased (to make up for the gas spring effect in the compressor). This is done by increasing the thickness of the springs and altering the spiral geometry.

3.2 GAS BEARING COMPRESSOR

During this program, STI modified their gas bearing compressor which was utilized in their

Stirling cycle applications for integration and operation with the pulse tube system. The linear motor approach was changed to facilitate an external coil. This system utilizes a pressurized gas space inside the piston to provide a cyclical flow of pressurized gas to the clearance gap between the piston and the cylinder wall thus centering the piston by hydrodynamic forces. This prevents rubbing and wear between the piston and cylinder. The linear motor for this design was a new approach and subsequent testing of the compressor integrated with the pulse tube indicated poor motor efficiency resulting in low PV powers delivered to the working gas and subsequent poor cooling performance. Work is underway to resolve this poor motor efficiency but this has not been resolved at this time.

The basic specifications of the compressor are summarized in *Figure 3-7*.

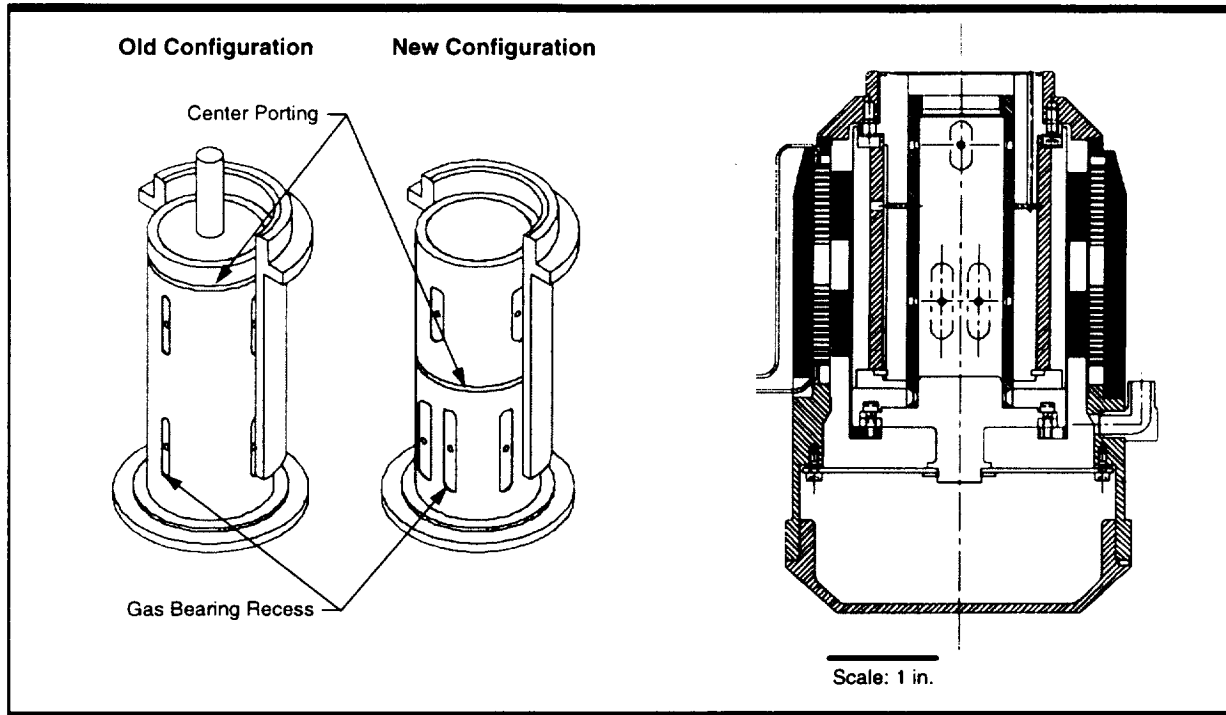
The cross section of this design is shown in *Figure 3-8*.

This layout drawing shows pressurized piston interior along with the gas ports which allow gas flow into the gap between the piston and cylinder wall during operation. The principle design characteristics of the linear motor are summarized in *Figure 3-9*.

Testing of the compressor system was carried out with a simulated pulse tube volume. Some difficulties were encountered with overheating and piston centering resulting in some modifications of the compressor. In tests at LM integrated with the pulse tube the compressor provided stable performance with

• Operating Speed = 50-60 Hz
• Piston Diameter = 1.25 inch (31.8 mm)
• Max. Stroke P-P = 0.538 inch (13.68 mm)
• Swept Volume = 0.66 inch ³ (10.8 cc)
• Moving Mass = 0.307 lb (139 grams)
• Overall Size:
- Diameter = 3.13 inches (8.0 cm)
- Length = 6.88 (17.5 cm)
- Weight = 4.25 lbs (1.93 Kg)

Figure 3-7. Gas bearing compressor specifications



LCC-029

Figure 3-8. Gas bearing compressor configuration

adequate piston centering, however, motor efficiency was well below requirements.

Tests are continuing at STI in an attempt to improve the motor efficiency of this system.

3.3 PULSE TUBE COLDHEAD

3.3.1 Initial Design- In-line Pulse Tube

The initial requirements for the pulse tube coldhead were 4W at 74K with a reject temperature of 330K. The pulse tube was designed for the STI K-Compressor, which was simultaneously being designed and developed. David Gedeon performed most of the initial work, and several iterations were required to explore various configurations before arriving at the final design.

- | |
|-------------------------------|
| • Dual moving magnets |
| • Stationary back iron |
| • Two external coils |
| • NeFeB magnet material |
| - 17 Gage wire, 45 turns/coil |

Figure 3-9. Linear motor design for gas bearing compressor

The three main areas of analytical investigation were:

- **Metal fiber vs. polyester fiber regenerator.** Because of low cost manufacturing requirements, only metal and polyester fiber regenerators were evaluated. The computer simulations indicated that the metal fiber regenerator would provide the better thermodynamic performance.
- **Concentric vs. in-line configuration.** The concentric configuration simplified integration of the pulse tube with the existing STI dewar. However, the predicted cooling power of the co-axial was about 3W, compared to 4 W predicted for the in-line configuration. The in-line configuration was then baselined, and STI designed a busbar link arrangement to integrate the in-line pulse tube with the dewar. With this arrangement, the pulse tube was completely external to the dewar.
- **DC flow control.** The computer simu-

lations indicated that the double inlet configuration could result in a dc flow circulation that could seriously degrade the performance of the pulse tube. Simultaneously, tests at NIST and at Lockheed indicated strong evidence for such flows. To cancel this flow, Gedeon suggested an asymmetric orifice for the secondary inlet where the pressure drop would not be symmetric with the flow direction. Using tables of loss coefficients for tapered orifices, an asymmetric orifice was designed to cancel the dc flow.

Heat exchangers were also designed. A copper fin heat exchanger was designed for the aftercooler, a copper screen exchanger for the cold heat acceptor, and a sintered bronze powder exchanger for the orifice rejector. Also

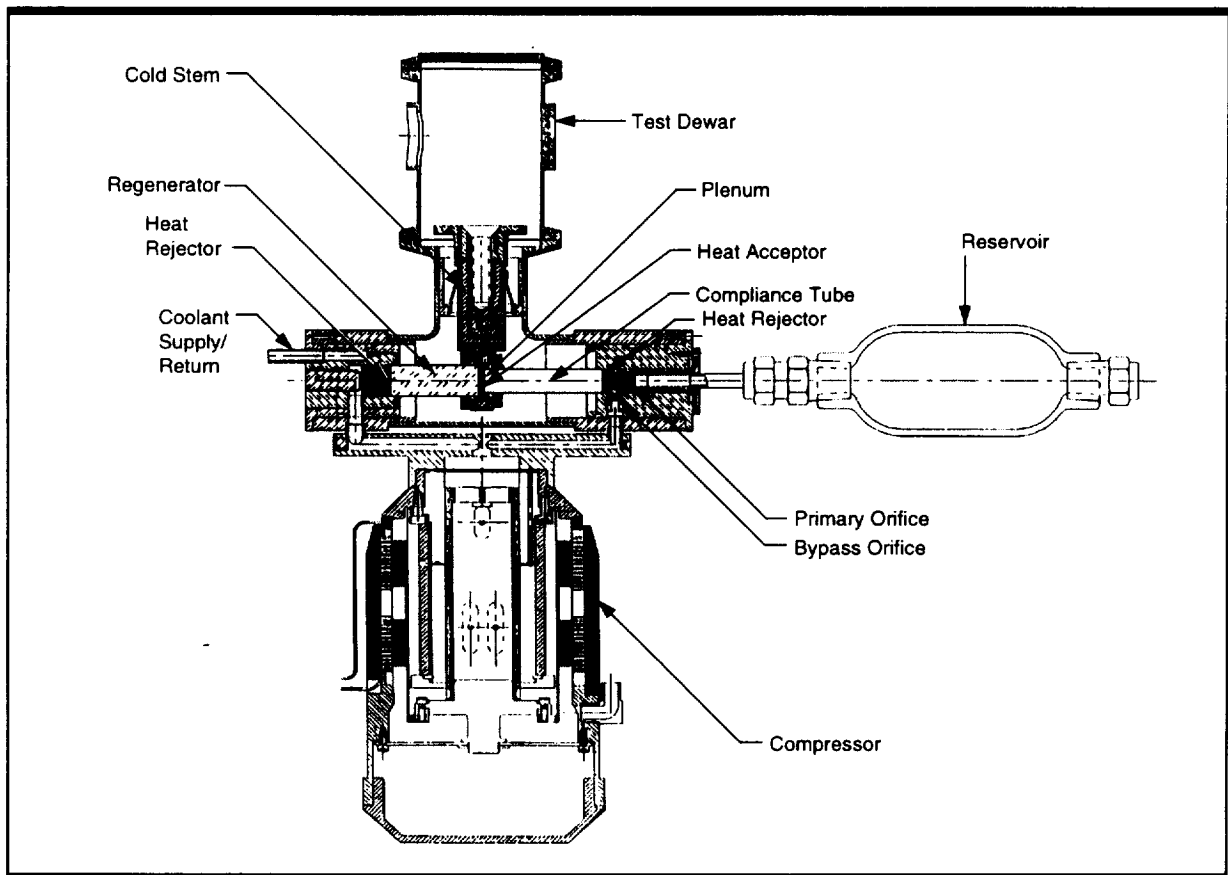
designed was a sintered bronze impedance for the primary orifice.

The layout of this original design is shown in *Figure 3-10*, and the design parameters listed in *Figure 3-11*.

3.3.2 Fabrication of the In-line Pulse Tube

LMMS proceeded to fabricate a version of this in-line pulse tube. Copper screen heat exchangers were substituted for the original copper fin main rejector and sintered bronze orifice rejector. A metering valve was substituted for the sintered bronze main impedance.

To control dc flows, a dual parallel metering valve arrangement was used, shown schematically in *Figure 3-12*. Metering valves have an inherent pressure drop asymmetry with flow direction so mounting these valves in parallel but with the needles oriented in opposite direc-



LCC-022

Figure 3-10. Original integration design with in-line pulse tube

General
Frequency: 59 Hz Pressure: 2.43 MPa Cold Helium Boundary Temperature: 74 K Warm Helium Boundary Temperature: 333 K
Compressor
Reciprocating Mass: 0.346 kg Piston Amplitude: 5.0 mm (10 mm peak to peak) Piston diameter: 25.1 mm (0.988 inch) Compression Volume: 3.62 cm ³ Connecting Duct Length: 70 mm (2.76 inches) Connecting Duct Diameter: 4.6 mm (0.181 inch)
Main Heat Rejecter
Main Rejecter Length: 10 mm (0.393 inch) Channel Width: 0.128 mm (0.005 inch) Channel Height: 3.18 mm (0.125 inch) Fin Thickness: 0.076 mm (0.003 inch)
Regenerator
Regenerator Material: Stainless steel Regenerator Length: 29.8 mm (1.173 inch) Regenerator Canister Inside Diameter: 10.6 mm (0.417 inch) Regenerator Canister Wall Thickness: 0.128 mm (0.005 inch) Regenerator Porosity: 0.87 Fiber Diameter: 8.0 microns (0.000315 inch)
Transition Plenum
Transition Plenum Material: Copper screen Transition Plenum Configuration: Single layer Transition Plenum Diameter: 10.6 mm (0.417 inch) Transition Plenum Screen Mesh: 16 wires per inch in both directions Transition Plenum Wire Diameter: 457 microns (0.018 inch)
Heat Acceptor
Heat Acceptor Material: Copper screen Heat Acceptor Length: 1.0 mm (0.039 inch) Heat Acceptor Diameter: 8.1 mm (0.319 inch) Heat Acceptor Porosity: 0.65 Heat Acceptor Wire Diameter: 114 micron (0.0045 inch)
Compliance Tube
Compliance Tube Length: 40.2 mm (1.583 inches) Compliance Tube Inside Diameter: 8.1 mm (0.319 inch) Compliance Tube Wall Thickness: 0.097 mm (0.004 inch)
Orifice Rejecter
Orifice Rejecter Material: Sintered bronze powder Orifice Rejecter Length: 3.2 mm (0.125 inch) Orifice Rejecter Diameter: 8.1 mm (0.319 inch) Orifice Rejecter Porosity: 0.39 Orifice Rejecter Particle Diameter: 84 microns (0.0033 inch)
Primary Orifice
Primary Orifice Material: Sintered bronze powder Primary Orifice Length: 7.1 mm (0.279 inch) Primary Orifice Diameter: 4.76 mm (0.187 inch) Primary Orifice Porosity: 0.39 Primary Orifice Particle Diameter: 84 microns (0.0033 inch)
Bypass Orifice
Bypass Orifice Configuration: Cylindrical, sharp edge Bypass Orifice Diameter: 1.05 mm (0.041 inch) Reservoir Volume: 50 cm ³

Figure 3-11. Design parameters of the pulse tube coldhead

tions allows adjustment of the net asymmetry. LMMS has used this technique successfully in the testing of our Mark II pulse tube. This valving arrangement, plus the laboratory mounting configuration of the compressor, led to an excessively long transfer line and extraneous ducting which resulted in significant loss in efficiency.

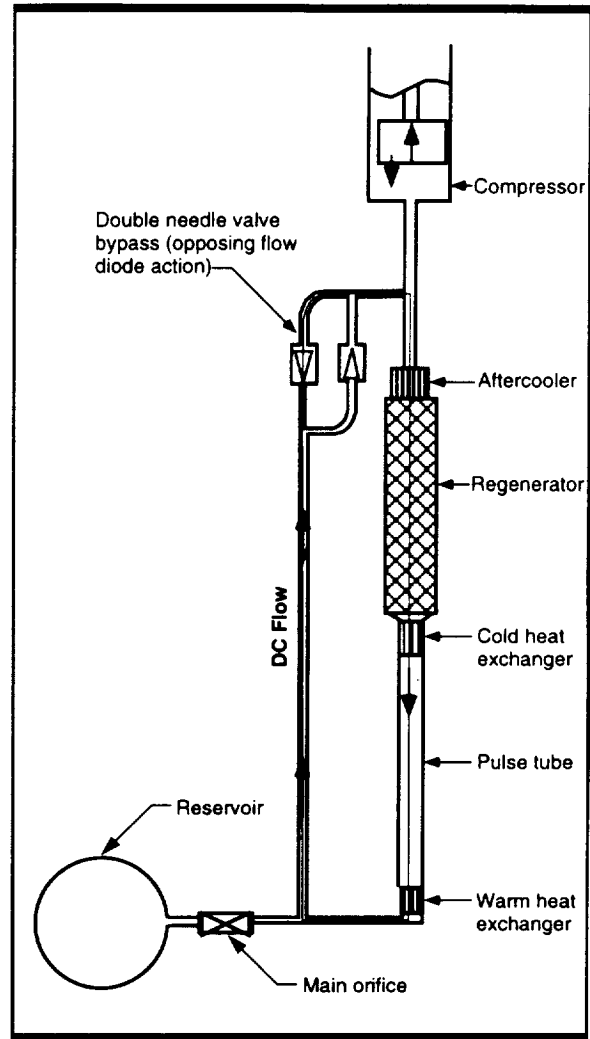


Figure 3-12. DC flow control

The initial tests were performed with LMMS's flexure bearing compressor. Heat rejection was by means of chilled water circulating through copper tubing clamped to both the compressor and the main rejecter.

Since the pulse tube was designed for the STI K-compressor, matching it to the LMMS flexure bearing compressor was somewhat problematic due to the large difference in moving masses, with the LMMS compressor having a 4.5X greater moving mass compared to the STI compressor. The solution was to use a large compression space void volume as an impedance match. To validate this technique,

we tested the flexure-bearing compressor/pulse tube combination with and without the large void volume, and the results demonstrate that the void volume configuration resulted in higher efficiency. Despite this, the flexure-bearing operating frequency of 40Hz to 45 Hz was still lower than the original design point of 59Hz, which resulted in further reduction in coldhead efficiency.

Test results are described in Section 4.2.1.

3.3.3 Design and Fabrication of the Concentric Pulse Tube, Filter Dewar Integration

As discussed in Section 4.2.1, this pulse tube demonstrated 2.5 W of cooling at 74K with 193 W of input power. To demonstrate cooling of the STI filter package, LMMS fabricated a concentric version to facilitate integration into the dewar. The essential dimensions, the regenerator cross section and length, and the pulse tube volume, were kept the same. The pulse tube aspect ratio was slightly altered to match the overall pulse tube and regenerator lengths. The coldhead was directly attached to the compressor, eliminating the transfer line, and the excessive external ducts were eliminated. Metering valves were again used for the primary orifice and the dual opposed metering valves were used for dc flow control in the secondary orifice. These were brazed directly into the copper coldhead with minimal lengths of tubing. The design accommodated STI's flanged arrangement for insertion of the coldtip into the dewar. To achieve slightly higher performance, titanium instead of stainless steel was used for the coldtip. The copper compressor head and compressor body was cooled with circulating chilled water.

The pulse tube length was significantly shorter than the length of the insertion hole in the STI filter dewar since the dewar was designed to accommodate the STI Stirling-cycle cooler. Thus, a link was required to

provide the thermal path from the end of the coldtip to the cold junction of the dewar. Originally, a solid copper bar with thermal grease press contacts at both the dewar and coldtip ends were used. However, thermal contact was lost during cooldown due to differential contraction of the copper bar and the inconel dewar walls, despite a designed-in preload of the link. A flexible copper link was then developed consisting of three annealed copper ropes soft soldered into flanges. One flange was soft soldered directly to the coldtip of the pulse tube, while the other end contacted the dewar with a thermal grease press fit joint. This arrangement proved successful and allowed cooling of the dewar.

A layout of the final cryocooler-dewar arrangement is shown in *Figure 3-13* and details of coldtip/dewar arrangement is shown in *Figure 3-14*.

3.4 ELECTRONIC CONTROLLER

During this program we (LMATC) designed an electronic controller to operate the cryocooler. Various components were breadboarded and we purchased two electronic controllers from Advanced Motion Controls, Inc., Princeton, WI.

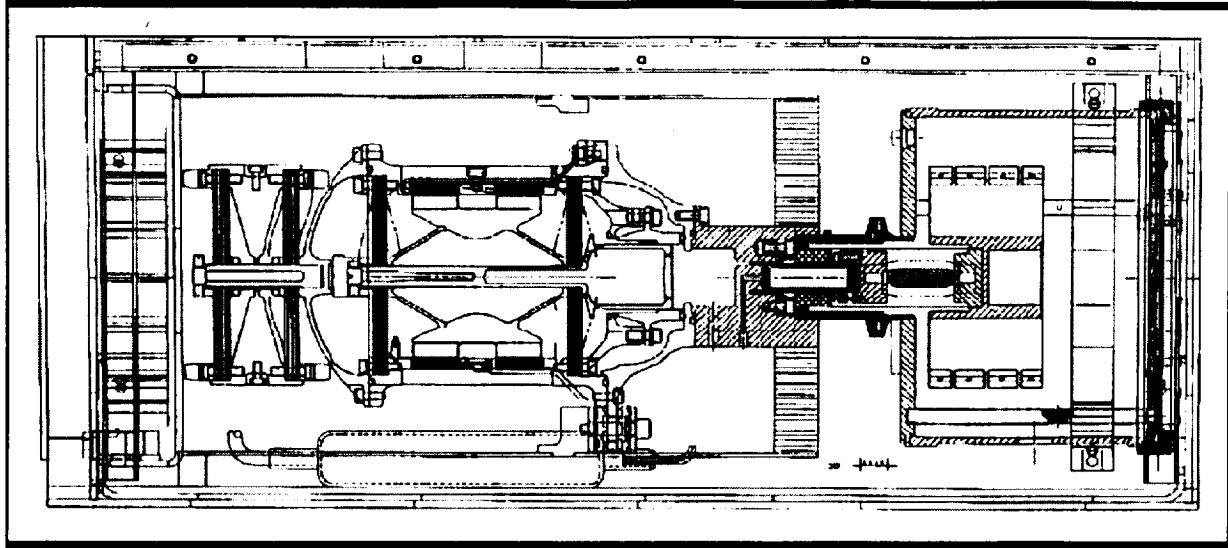
These units included a two phase motor controller with DSP (TM 5320C51) and a 16-bit A/D converter.

The system utilized control loops for both stroke control and temperature control.

The specifications of the controller are summarized in *Figure 3-15* and a photograph of the system is shown in *Figure 3-16*.

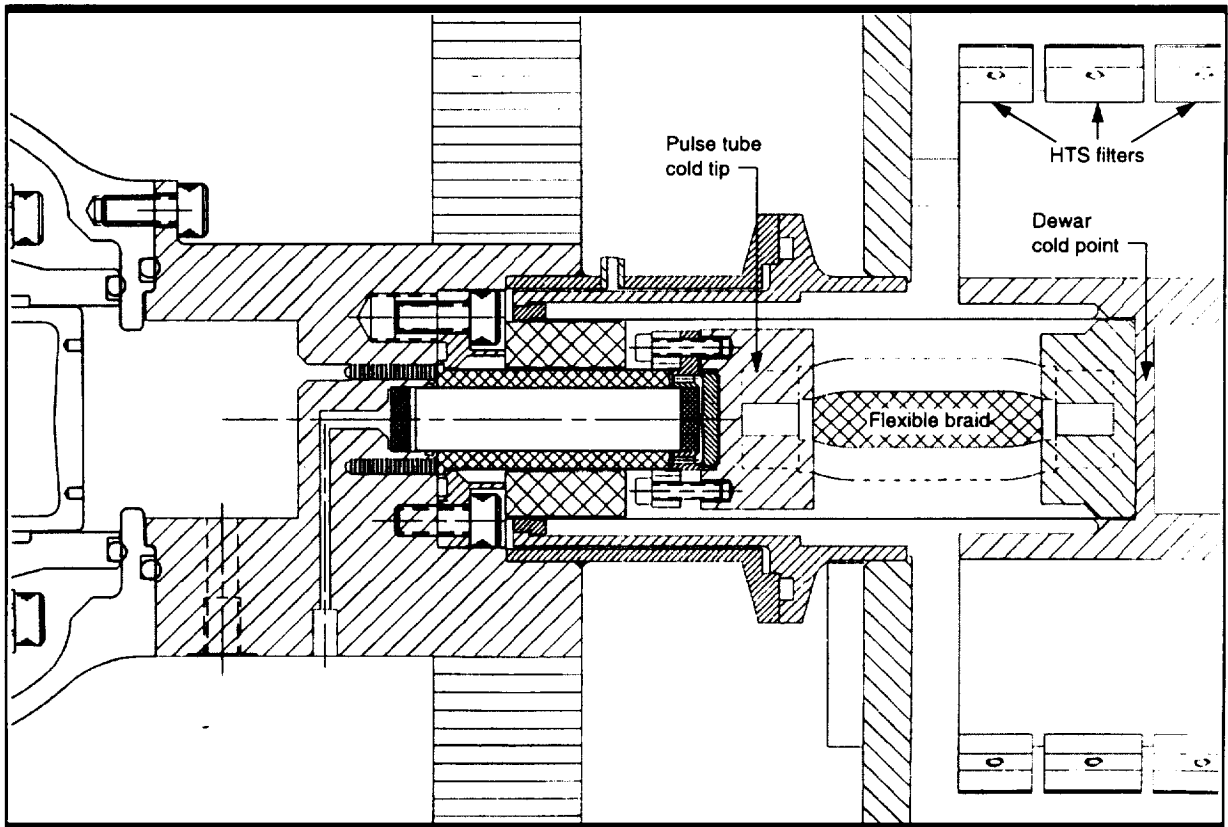
EPROMS were loaded with the LM specified software and 50 Hz current output.

Some difficulties were encountered with the software and while it was intended to drive the compressor with this controller, this has not been accomplished to date, due to limitations on funding and schedule.



LCC-002

Figure 3-13. Layout of flexure bearing pulse tube integrated with HTS filter dewar



LCC-003

Figure 3-14. Interface details between coaxial pulse tube and dewar

Operating Temperature	-10 - 60 deg C
Humidity	95%
Power Input	+22 to +32 vdc
EMI	Meet FCC Part 15 Class A Radiated
Duty cycle	100%
PWM amplifier efficiency	95%
Current Capacity	20 amps cont. (10 amps cont. option)
Peak Current Capacity	30 amps pk (15 amps pk)
Nominal Supply Voltage	28 vdc
Current Mode configuration	Bandwidth 2 Khz
Protection Circuits:	Over current, over voltage, over temperature, output shorts
RS232 serial interface 16 bit integer processor (TMS320C51) Additional on-board ram and flash ram 16 bit A/D with multiplexed inputs Cryogenic Temperature sensor Position sensor monitoring Motor temperature monitoring C software control implementation	

Figure 3-15. Specifications for electronic controller for pulse tube cryocooler



LCC-031

Figure 3-16. Electronic controller to drive compressor

4.0 TESTS

Over the course of this program, we tested three compressors- an LMMS flexure bearing compressor with a 34 mm diameter piston (Compressor A), a second LMMS flexure bearing compressor with a 30 mm diameter piston (Compressor B), and an STI gas bearing compressor. Characterization tests were performed with a dead volume to simulate the pulse tube load, and cooling power tests were performed with the in-line pulse tube.

The concentric pulse tube was tested with Compressor B. The filter package cooling demonstration, was performed with the concentric pulse tube driven by Compressor B. The test matrix is shown in *Figure 4-1*.

A detailed report of the compressor dead volume tests and the in-line pulse tube tests has been submitted to NASA GFC, so in this report we summarize the main results of these tests.

4.1 TEST APPARATUS

The pulse tubes and compressors were fully instrumented for characterization and diagnostic purposes. Coldstage temperatures were monitored with calibrated PRT thermometers, and ambient temperatures were monitored with thermocouples. Thermocouples were bonded to the walls of the coldtip to monitor the temperature profile for diagnosing dc

flows. Pressure transducers monitored the compression space, pulse tube, and reservoir volume pressures. Kaman eddy current sensors monitored the piston position. Pressure and position data was digitized with a digital oscilloscope, and stored on a computer for processing.

The compressor was driven by a linear amplifier with a Wavetec signal generator as a signal source. The rms current, rms voltage, and total power into the compressors were monitored with a Valhalla power meter.

The dead volume apparatus for compressor characterization consisted of an adjustable volume and a valve in series with a second, large reservoir volume. The valve and volume adjustment allowed variation of the gas spring and total dissipation as seen by the compressor. PV delivered by the piston was calculated from the measured piston position and pressure amplitude. PV into the reservoir volume was calculated from the compression space pressure amplitude and the mass flow into the reservoir volume, as determined by the pressure amplitude in the reservoir. The PV delivered by the piston was always slightly higher than the PV into the reservoir because of seal blowby loss, and gas bearing loss in the case of the STI compressor.

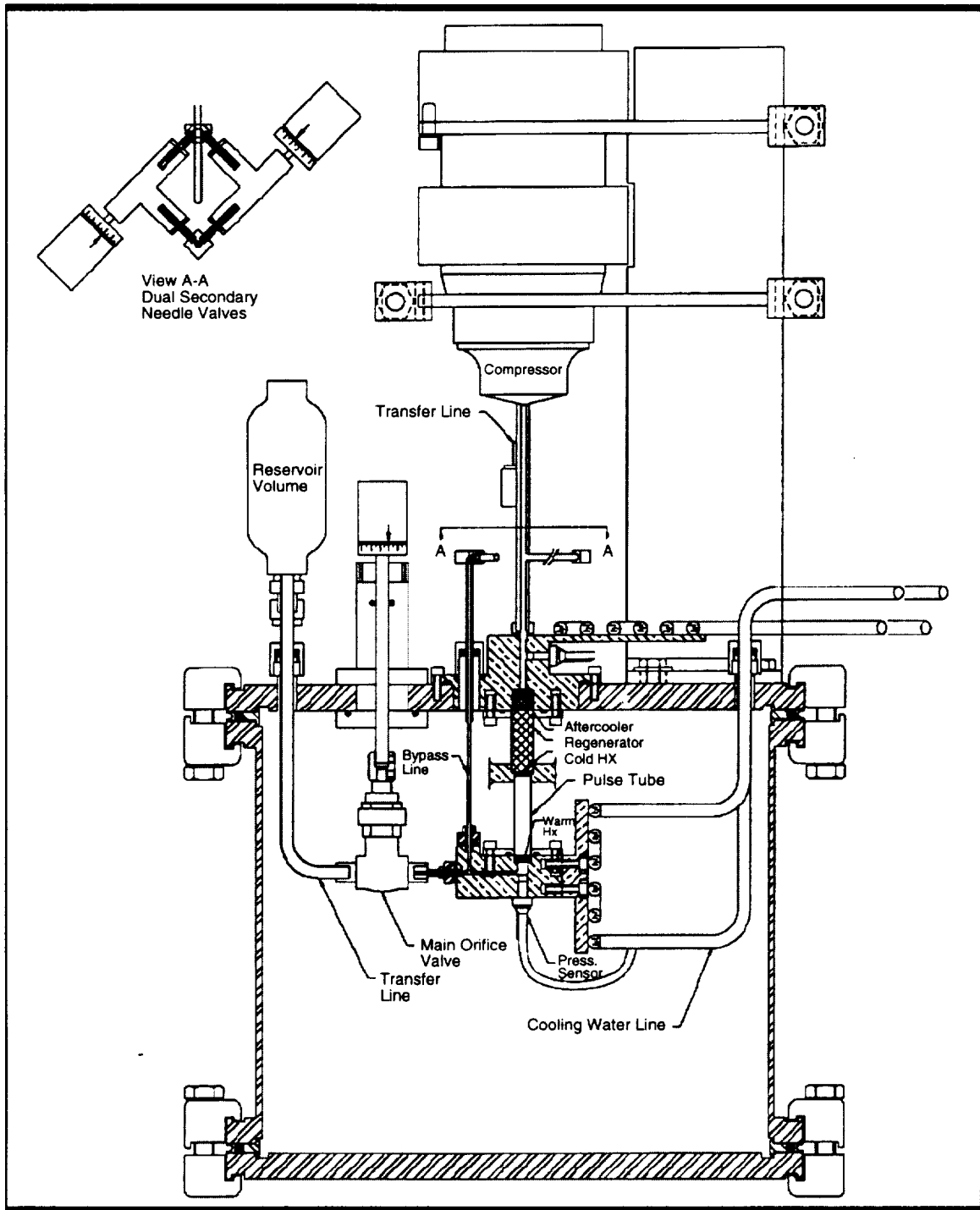
Within experimental accuracy, the PV power and I^2R power equaled the total power, indicating that all significant losses were accounted for in the flexure bearing compressors. A slightly larger power discrepancy was observed in the gas bearing compressor, possibly suggesting eddy current or hysteresis forces. Dynamic force balance was also verified by summing the pressure force, spring force, moving mass inertia, and motor forces calculated from the digitized piston position and pressure data, and using motor force constants and spring constants from dc measurements.

Compressor	Pulse Tube	Test
LMMS Compressor A (34 mm dia piston)	None	Dead Volume
LMMS Compressor B (30 mm dia piston)	None	Dead Volume
STI Gas Bearing Compressor	None	Dead Volume
LMMS Compressor A (34 mm dia piston)	in-line	Cooling Performance
LMMS Compressor B (30 mm dia piston)	in-line	Cooling Performance
STI Gas Bearing Compressor	in-line	Cooling Performance
LMMS Compressor B	Concentric	Cooling Performance
LMMS Compressor B	Concentric	Filter Demonstration

Figure 4-1. Text matrix for concentric pulse tube

The in-line pulse tube was tested in a large vacuum can, with the coldhead penetrating the vacuum wall, and the compressor mounted external to the can. A

schematic of the test apparatus is shown in Figure 4-2. The concentric pulse tube was tested with a small vacuum shroud over the coldtip.



LCC-005

Figure 4-2. Test apparatus for in-line pulse tube

4.2 TEST RESULTS

The dead volume characterization tests on both the flexure bearing compressors and the gas bearing compressor, as well as thermodynamic tests with both compressors with the in-line pulse tube, have already been described in great detail in a report submitted Dec. 1996. These tests were quite extensive as they explored performance over a wide parameter space. Here, we summarize the key results of the thermodynamic tests.

4.2.1 Flexure Bearing Compressor In-line Pulse Tube Test

The flexure-bearing compressor in-line pulse tube tests were performed with three configurations: Compressor A with a 34 mm diameter piston, 12.8 cc void volume, Compressor A with a 34 mm diameter piston, 1.5 cc void volume, and Compressor B, 12.8 cc void volume. Load lines from these tests are shown in *Figure 4-3*. Data were taken at constant

stroke with varying total compressor powers, with about 168 - 178 W for Compressor A, 1.5 cc void volume; 190 W for Compressor A, 12.8 cc void volume; and 196-203W for Compressor B, 12.8 cc void volume. For a direct comparison of the thermodynamic efficiency, the compressor specific power is plotted in *Figure 4-4*. These data show that the compression space void volume matching scheme resulted in better overall efficiency.

Figure 4-5 summarizes the performance of these three configurations at the design point of 74K. As seen, the configuration with the minimum void volume provided very little cooling, while the configurations with the large void volumes produced over 2.5 W of cooling. *Figure 4-6* summarizes the power balance for Compressor B at the 74K point. The individually measured powers all sum to the measured total power, indicating that all motor related losses have been accounted for. The entry

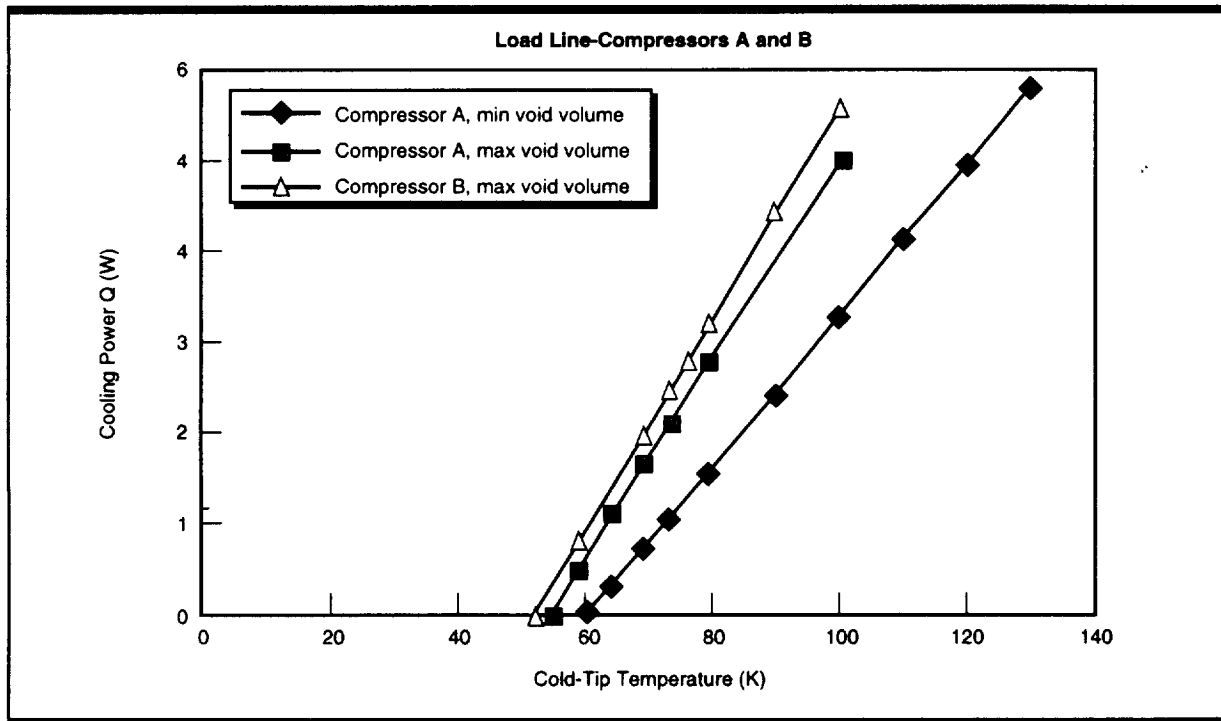
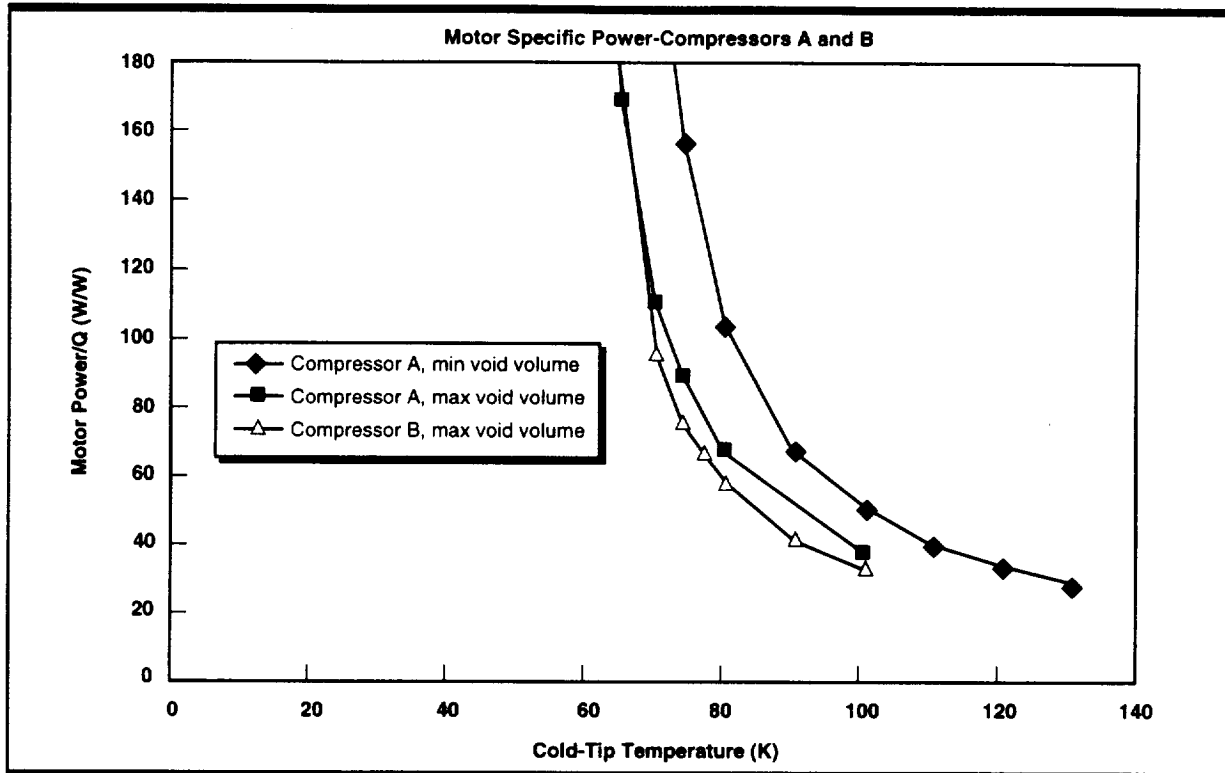


Figure 4-3. Load lines for in-line pulse tube



LCC-007

Figure 4-4. Specific power for in-line pulse tube

under "Integrated Residual Power," is of unknown origin, possibly eddy current drag, and is calculated by integrating the residual force from a force balance plot. The contribution is small, only 3% of the total power, and could be due to experimental inaccuracy.

Compressor	A	A	B
Void Volume (cc)	1.5	12.8	12.8
Q@74 K (W)	1.07	2.6	2.52
Total Input Power (W)	173	193	193
PV Power (W)	N/A	N/A	103

Figure 4-5. Performance summary of in-line pulse tube

Power-Balance: Compressor B	
Q@74 K	2.5
Measured PV Power (W)	103
i ² R Power (W)	84
Integrated REsidual Power (W)	5.8
Total (W)	192.8
Total Measured Input Power (W)	193

Figure 4-6. Power Balance of Compressor B

4.2.2 Gas Bearing Compressor In-line Pulse Tube Test.

The STI gas bearing compressor performance was poor in both pulse tube and dead volume tests. Only 0.387 W of cooling power at 74K was achieved with about 209 W of total power into the compressor. PV power for this operating point was only 63 W, indicating significant motor losses. Force balance and power balance measurements, both with the pulse tube and dead volume, confirmed the poor motor performance. Figure 4-7 summarizes the results of the cooling power tests, and more detail on all tests were provided in the Dec. 1996 report.

4.2.3 Flexure Bearing Compressor Concentric Pulse Tube Tests

As described in Section 3.2.3 a concentric version of the pulse tube was fabricated. We removed the transfer line, a significant amount of the external flow ducts, and replaced the

Void Volume (plug)	Charge Pressure (MPa)	Freq (Hz)	Temp (K)	Cooling Power (W)	Peak Stroke (mm)	Compressor Power (W)	PV (W)	Motor Efficiency PV ÷ Total
Min	2.0	54.25	69.68	0.000	3.92	204	63	0.309
Min	2.0	54.25	74	0.387	3.87	209	63	0.301
Max	2.5	55.34	76	0.000	4.65	202	53	0.262

Figure 4-7. STI compressor/pulse tube cooling tests

stainless steel tube walls with titanium. These changes significantly improved the thermodynamic efficiency. On the other hand, epoxy was used initially to bond the copper cooling water lines to the compressor head, which proved to be inadequate and degraded performance. Overall, the efficiencies were similar between the in-line and concentric pulse tube.

The comparison of the load lines of the concentric pulse tube and the in-line pulse tube is shown in Figure 4-8. The concentric pulse tube data was with 180 W of total compressor power. While there are enough differences between the in-line and concentric configurations to prevent this from being a one-to-one comparison, the data do suggest that concen-

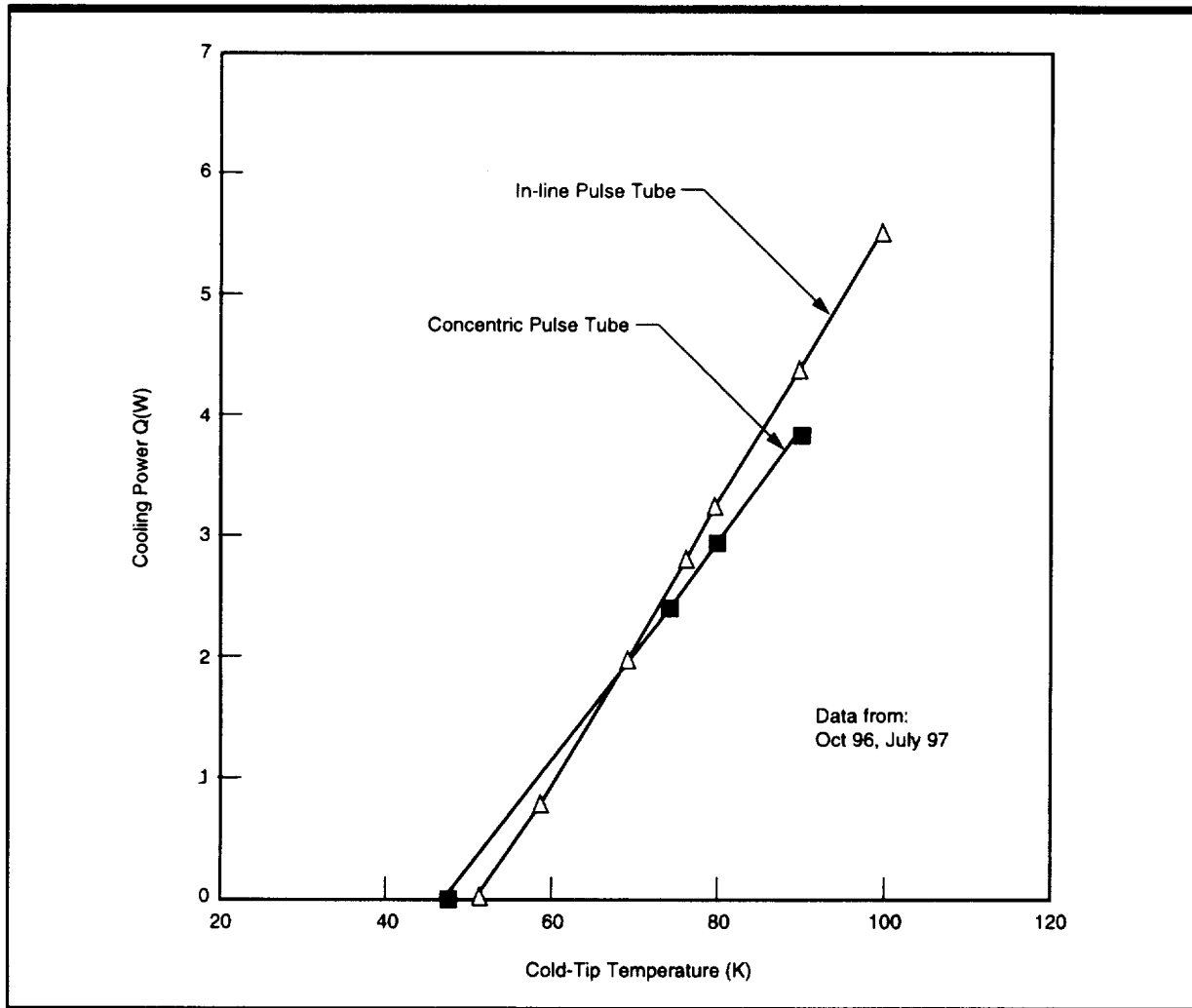


Figure 4-8. Comparative testing on concentric and in-line configuration (second design)

tric pulse tube performance can be comparable to that of in-line pulse tubes.

Several hardware problems were encountered during the development of the coaxial pulse tube. The initial cooldown reached only 130K, and we diagnosed the following problems:

- Our bypass valves were inadvertently plugged with braze.
- Non-concentricity of the pulse tube and regenerator tube resulted in gaps between the regenerator mesh and the walls, resulting in blowby losses.
- The demountable coldhead design required an internal seal between the pulse tube and the compressor head to prevent flow from bypassing the regenerator. While the double inlet configuration has a secondary that is in parallel with this leakage path, our concern was that an ill defined leak could be the source of significant dc flow generation.
- The flow straightening at the cold end of the pulse tube was insufficient.

Corrective action was taken on all of these. The compressor head was rebuilt, with care taken not to replug the valves. A second set of metal felt regenerator disks was cut slightly oversized to insure sealing at the edges. A small o-ring with a metal retainer was used to provide the internal seal at the warm end of the pulse tube. The pulse tube coldhead was rebuilt with additional screens at the cold end.

With all these corrections in place, the pulse tube cooled to a no-load temperature of 51K, and the load line in *Figure 4-8* was taken. This pulse tube cooled rapidly, reaching 77K within a few minutes, and was very repeatable. The dual needle valve technique was used to cancel dc flows, and once the valves were set, the pulse tube performance was consistent from cooldown to cooldown, and demonstrated temperature stability over the duration

of several hours, the longest period of time over which we ran these tests.

4.2.4 Concentric Pulse Tube-Filter Package System Test

Upon successful testing of the concentric pulse tube, we proceeded to integrate the coldtip to the STI filter dewar for the system demonstration. Despite the consistent and stable behavior of the pulse tube during the previous tests, cooling the dewar initially proved problematic. The coldtip would slowly cool because of the large thermal mass of the filter package, and typically between 100 K and 130 K, the temperature would bottom out and begin to rise.

While we did not clearly identify the specific mechanism that prevented the cooldown, we addressed all potential mechanisms that could affect performance and corrected each one. These were:

- **Contamination:** We vacuum baked the coldtip and compressor head for several hours prior to assembly.
- **Vacuum leak:** There was a small leak into the vacuum jacket of the coldtip from the o-ring seal between the coldtip to the compressor head. While pressure should not have produced a sizable heat leak, we sealed that joint with epoxy.
- **Compressor head heat sink:** Originally, the cooling water lines around the coldhead were bonded down with epoxy. We cleaned off the epoxy and soft-soldered the copper lines to the coldhead, greatly improving the thermal contact and significantly lowering the rejection temperature.
- **Improved thermal link:** the original thermal link between the coldtip and the dewar coldstage was a solid copper bar. As described in Section 3.2.3, this proved problematic and was replaced with a flexible braided rope link.

Once these corrections were made, the filter package cooled to the required temperature of 77 K, and filter response measurements were made. Total compressor power required for these tests were between 125 to 130 W. The pulse tube compressor performance was very stable and well behaved. Excellent data on the filter performance was achieved and is shown in *Figure 4-13*. Photographs of the cryocooler packaged with the dewar are shown in *Figures 4-9, 4-10, 4-11, and 4-12*. The layout of the system is shown in *Figure 3-13*. Details of the co-axial pulse tube-cold finger integration are shown in *Figure 3-14*.

4.2.5 Etched Foil Regenerator

Under IRAD support as part of cost sharing for this program, we tested several Etched Foil Regenerators (EFR), both in Stirling and Pulse Tube cryocoolers. The EFR is a regenerator fabricated by photoetching metal foils into a

particular pattern, then rolling the foil into a tight bundle. The final flow configuration is similar to parallel plates but with slits introduced into the plates for crossflow between the channels to prevent flow maldistribution. CFD analysis on the idealized EFR geometry indicated that the compactness factor is a factor of three higher than screens, which should result in a significant performance improvement in cryocooler performance.

The test matrix is shown in *Figure 4-14*, where the cooler and the comparison regenerators are listed. The comparison is made in terms of minimum temperature since in one case the EFR pulse tube did not reach even 105 K. In all cases, the screen regenerator showed superior performance.

Work at NIST where an etched foil regenerator was used as a replacement for screens in a pulse tube showed that the etched foils regen-

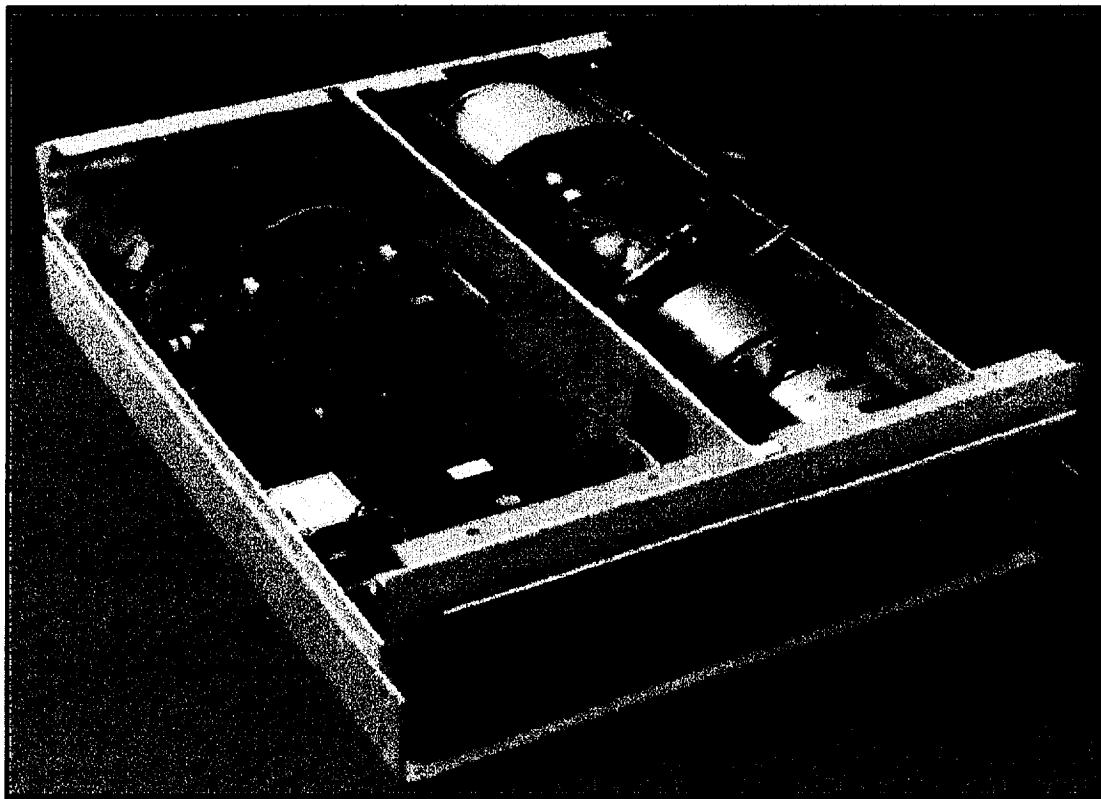
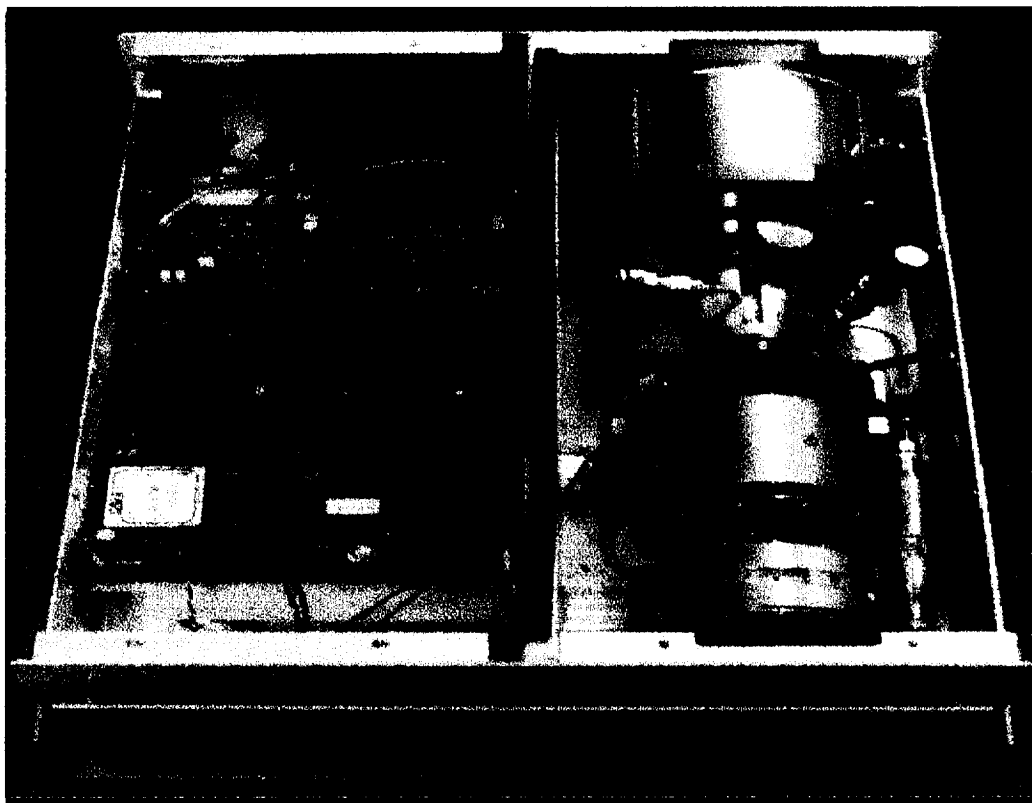
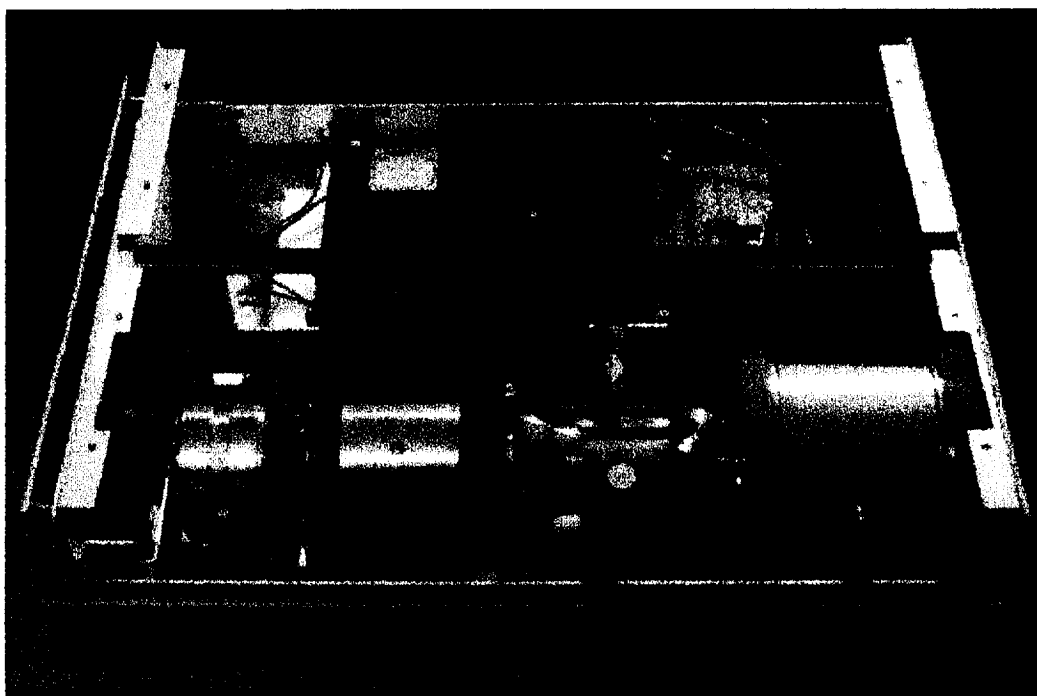


Figure 4-9. Flexure Bearing—concentric pulse tube integrated with STI HTS filter package



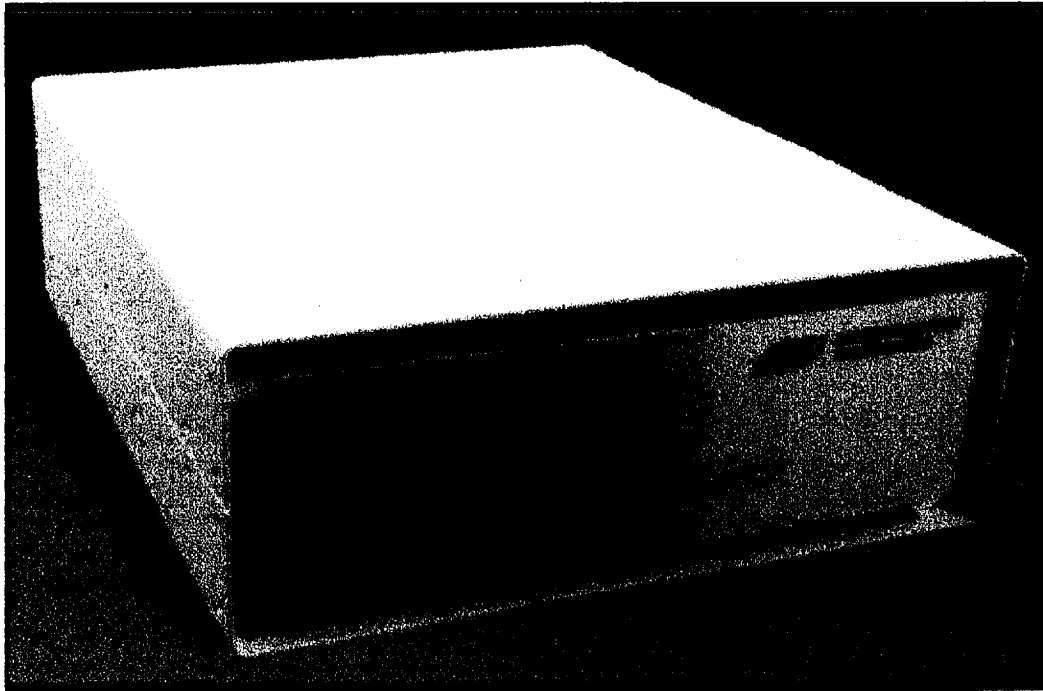
LCC-010

Figure 4-10. Flexure Bearing—concentric pulse tube integrated with STI HTS filter package



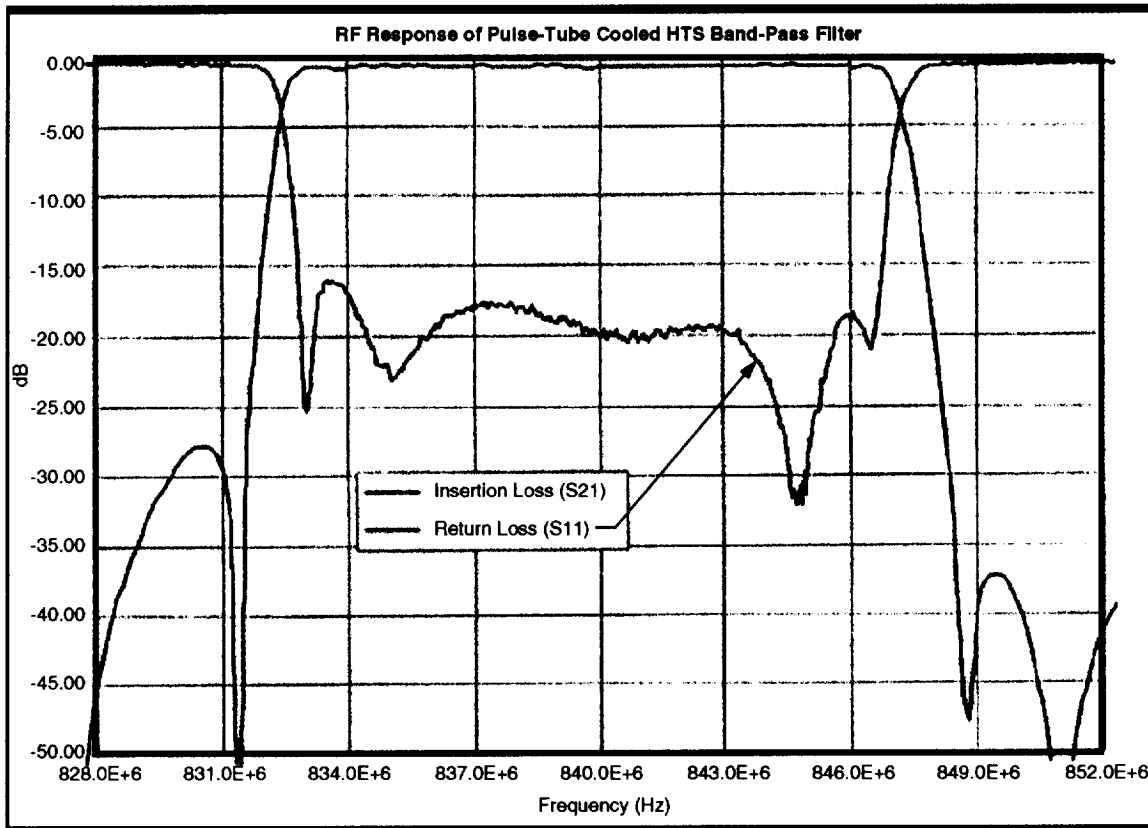
LCC-011

Figure 4-11. Flexure Bearing—concentric pulse tube integrated with STI HTS filter package



LCC-012

Figure 4-12. Flexure Bearing—concentric pulse tube integrated with STI HTS filter package



LCC-028

Figure 4-13. Measured RF response for HTS filter dewar—pulse tube cryocooler test

Cooler	Regenerator	Minimum Temp (K)
LMMS 1710C Stirling	#380 screens	22
LMMS 1710C Stirling	50 μ EFR #1	33
LMMS 1710C Stirling	50 μ EFR #2	41
LMMS Mark I Pulse Tube (NIST design)	#400 screens	69
LMMS Mark I Pulse Tube (NIST design)	50 μ EFR	105
LMMS Mark II Pulse Tube (LMMS design)	#400 screens	86
LMMS Mark II Pulse Tube (LMMS design)	30 μ EFR	55

Figure 4-14. Summary of tests comparing the etched foil generator with screens

erator resulted in higher cooling capacity. In reviewing the NIST data, it is clear that in that case, the screen regenerator was poorly optimized, so it was not a valid comparison of the etched foil vs. screens.

Based on our experience with the etched foil, we have concluded that the fabrication process is not sufficiently developed to produce the idealized geometry. First, the etching process is at the resolution limits of the particular photoetching technique used. The uniformity of the thickness and the control of the local geometry for our particular samples may not have been sufficient. Second, the process of rolling the foils resulting in uneven gaps between the foils. This problem was exacerbated in situations where several sheets of foil had to be joined to provide enough regenerator material to fill the cryocooler to be tested.

Since the analysis on the idealized geometry indicates a factor of three improvement over screens, the final product can still have a compactness factor significantly below predictions and still outperform screens. Our overall view is that the EFR concept therefore has potential, but will require further refinements in fabrication methods to outperform screens.

4.2.6 DC Flow Investigations

As discussed in Section 3.3.1, Gedeon's computer simulations indicated that the closed loop fluid path could allow for a dc flow circulation through the regenerator, as shown in

Figure 3-12. There are several mechanism that can generate dc flows from ac flows, and in fact, ac flow with an irreversible pressure drop is almost always likely to generate dc flows. This dc flow imposes a load on the coldstages since the flow is essentially unregenerated from room temperature to the cold stage. Thus, it can be a substantial parasitic load on the cooler. To study this behavior, we developed the dual opposed secondary needle valve technique shown in Figure 3-12 and described in Section 3.3.2.

Our first observation was the sensitivity of the temperature profile to the secondary settings, which shifted in a direction consistent with dc flow with directionality determined by the metering valves. This is illustrated in Figure 4-15. The dashed line profile corresponded to the maximum cooling power, and was obtained by adjusting both secondary valves to about a 4 to 3 ratio. We believe this to be the case where there is minimal dc flow. The squares correspond to having opened only that needle valve which, if the dc flow is in the direction of the needle, would generate flow from right to left in the figure. The triangles are data for the case where only the other needle valve is opened. As expected, if the dc flow is from the regenerator to the pulse tube, the warm dc flow from ambient imposes an additional load on the regenerator, increasing the local temperature, while in the pulse tube, the flow is cooled by the coldstage, the flows into the pulse tube, reducing the local temperature. While we have no direct measurement of the mass flows, we consider this compelling evidence for dc flows within the pulse tube.

These temperature profile shifts were accompanied by loss in cooling power. Figure 4-16 shows the cooling power and the accompanying regenerator and pulse tube midpoint temperatures as only one secondary valve is opened, and as both valves are opened simulta-

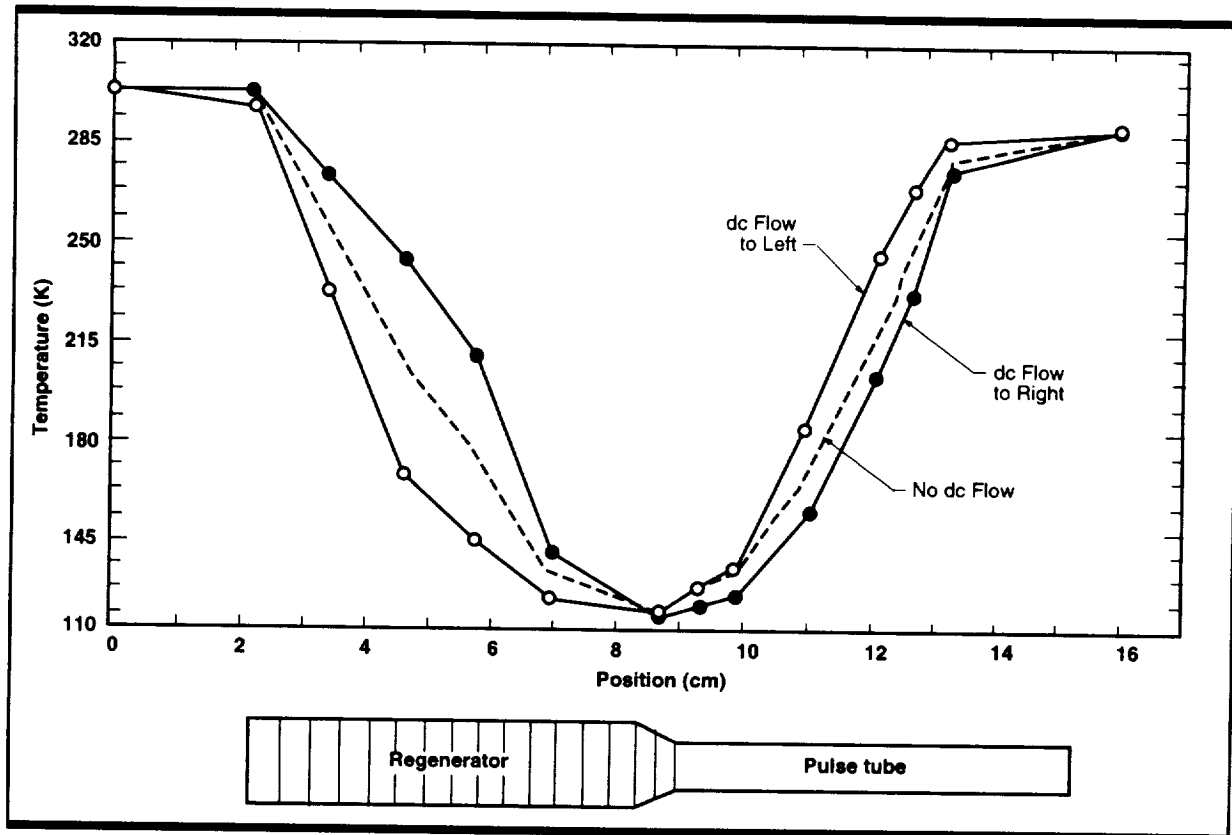


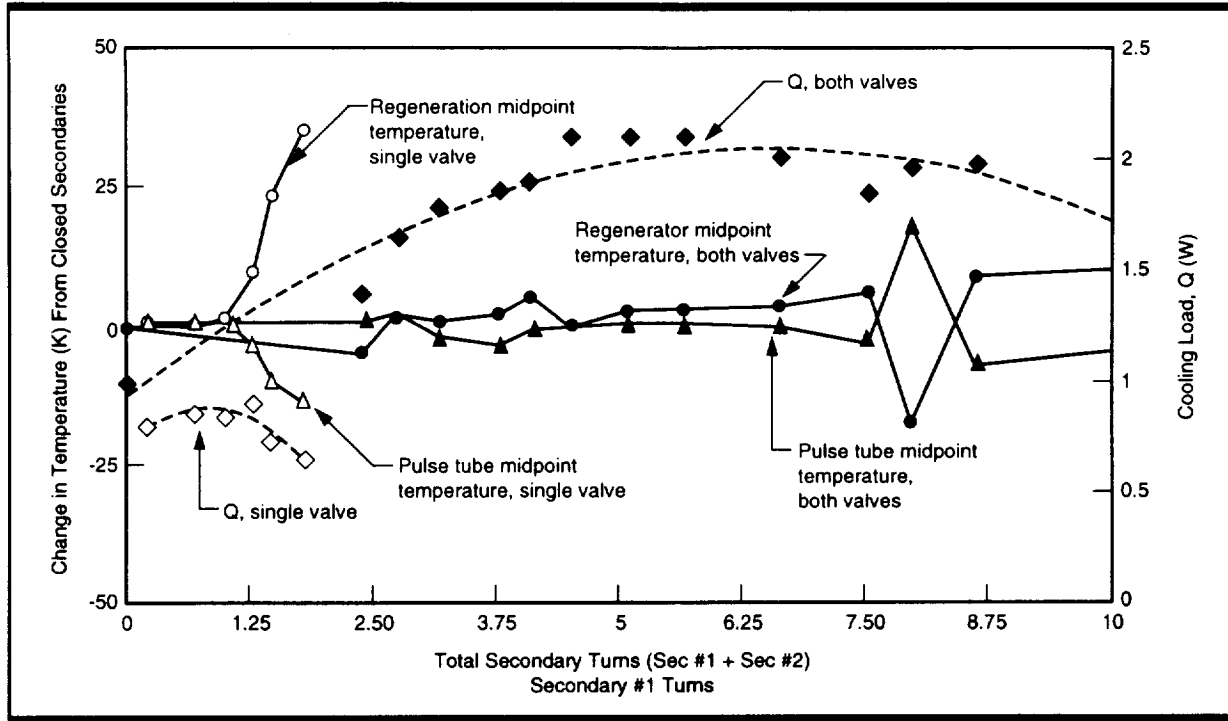
Figure 4-15. Regenerator/Pulse Tube Temperature Profile. The temperature profile clearly indicates the dc flow condition.

neously with the ratio adjusted to keep the midpoint temperatures constant. The horizontal axis is the number of secondary turns, and a striking difference in behavior is observed depending on whether one secondary is opened, or both are simultaneously opened.

Experimentally, each run is initiated with both secondaries closed, the primary open, and the temperature regulated well above the no-load temperature such that there is measurable cooling power. If only one secondary is opened, the regenerator midpoint temperature (open circle) remains constant, then abruptly increases once the secondary is opened past about 1 turn. The pulse tube midpoint temperature (open triangle) abruptly decreases at this point. This shifting of temperature is precisely the behavior depicted in Figure 4-15. The cooling power (open diamond), begins to

increase as expected from the double inlet effect, then begins to decrease at about the point where the regenerator and pulse tube temperature begin to deviate from the starting points. We interpret this as the onset of dc flows. If the other secondary only is opened, the same behavior is observed except that the pulse tube temperature increases and regenerator temperature decreases. When both needle valve are opened simultaneously, and the ratio of the number of turns adjusted to maintain the regenerator and pulse tube temperatures (filled circle and filled triangle) near the initial point, the cooling power (filled diamond) reaches higher values at substantially larger secondary openings.

From this, we have concluded that the dual needle valve technique can control and generate dc flows, and that the dc flows can



LCC-033

Figure 4-16. Cooling power and the accompanying regenerator and pulse tube midpoint temperatures degrade pulse tube performance. Regenerator and pulse tube temperature profiles also are a valuable diagnostic for this phenomenon. This dual needle valve technique was used in all of the tests in this program.

5.0 SYSTEM COST PROJECTIONS

5.1 FLEE BEARING COMPRESSOR

Piece Parts Manufacturing

Manufacturing methods for higher production quantities were evaluated for each piece part. With some investment in tooling for mass-production processes, such as investment casting and forging, parts costs can be dramatically reduced. With these higher-production processes, parts are produced to near net shape inexpensively, significantly reducing raw material and machining operation—the primary components of manufacturing costs. Other possible manufacturing methods include chemical milling and laser cutting, both of which are reproducible and accurate and also eliminate machining time.

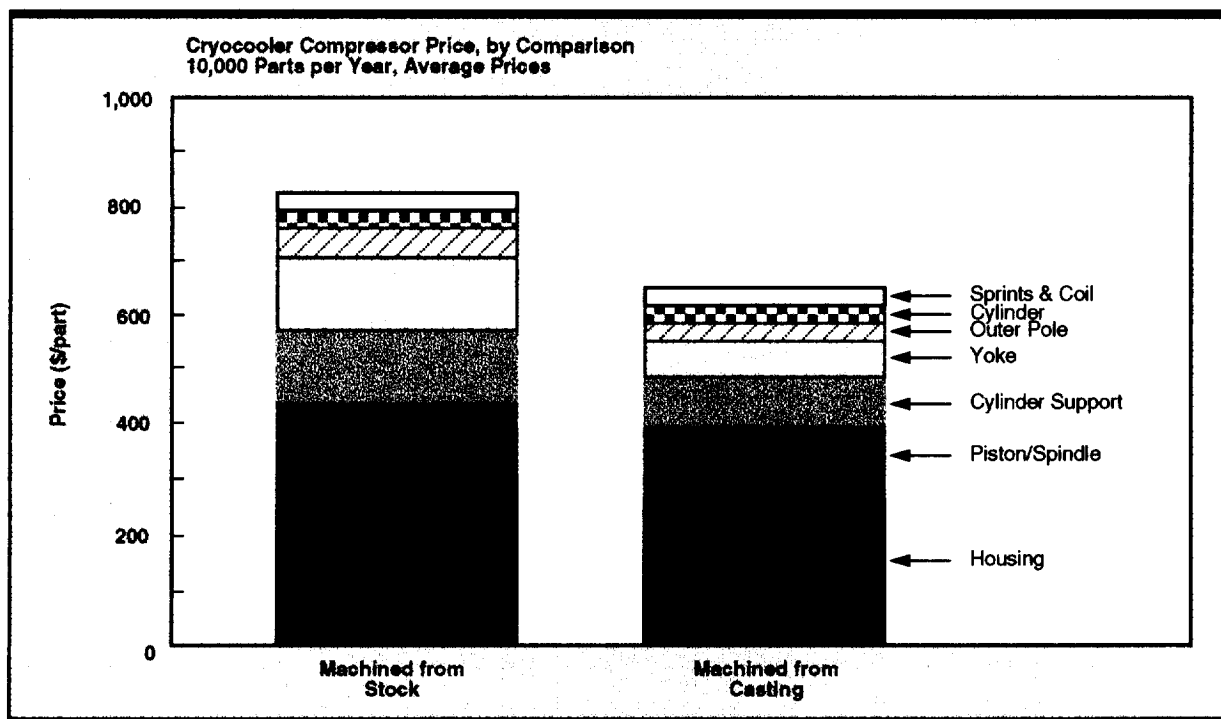
In order to estimate actual manufacturing costs in volume production, a study of piece part fabrication methods was commissioned by an outside consulting firm IBIS. The report from this study indicates that the major parts

cost for the compressor would range from \$700 to \$900 (depending on tooling investment) for build rates of 10,000 units/year (see *Figure 5-1*).

This study focused on the seven major piece parts that account for about 90% of the total parts costs. While cost per unit generally drops with increased volume, there was found to be a full 30% savings realized when casting processes are used to reduce machining labor (see *Figure 5-2*).

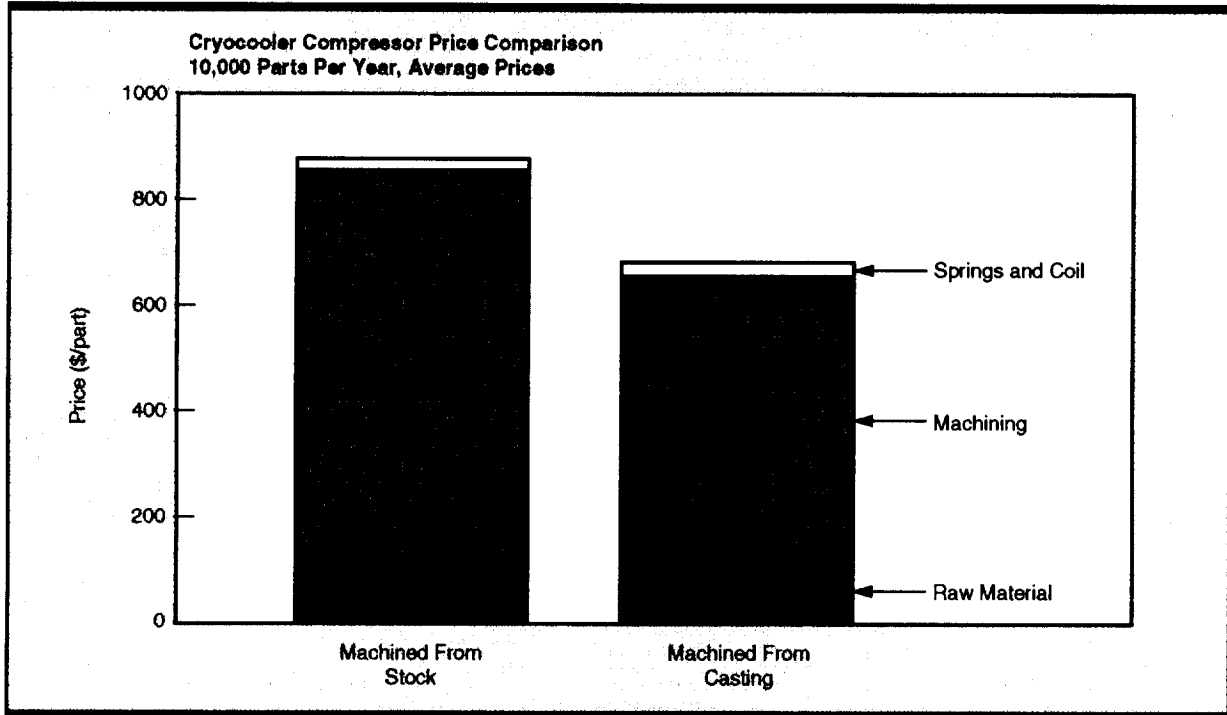
Assembly and Alignment

Assembly and alignment procedures now constitute a large part of the compressor manufacturing costs. Truing the linear bearing system and centering the clearance seal has traditionally been a long and tedious procedure, requiring highly skilled technicians who often resort to trial and error methods. Reducing this assembly to a simple, step-by-step procedure was necessary to meet cost goals. This is being accomplished in two



LCC-018

Figure 5-1. Composite prices by component



LCC-019

Figure 5-2. Composite prices comparing manufacturing approaches

stages, by simplifying assembly and by automating alignment.

Simplified Assembly. Assembly is simplified by eliminating adjustments in the linear bearing. The flexure bearing system is designed to be self-aligning upon assembly. Features integrated into the piece parts cause the piston/shaft to be centered in the single-piece housing, producing the required precision linear motion of the piston without the necessity for adjustments.

Automated Alignment. Automated alignment eliminates the need for operator skill. The final critical alignment of the piston and cylinder is accomplished by following a set procedure that determines the relative position of the parts and displays the results graphically in real time. The operator uses this display in conjunction with adjusting screws to move the cylinder into final alignment. High-resolution fiber-optic position sensors, which track part position, are already in use at Lockheed Martin. Microactuators with force feedback

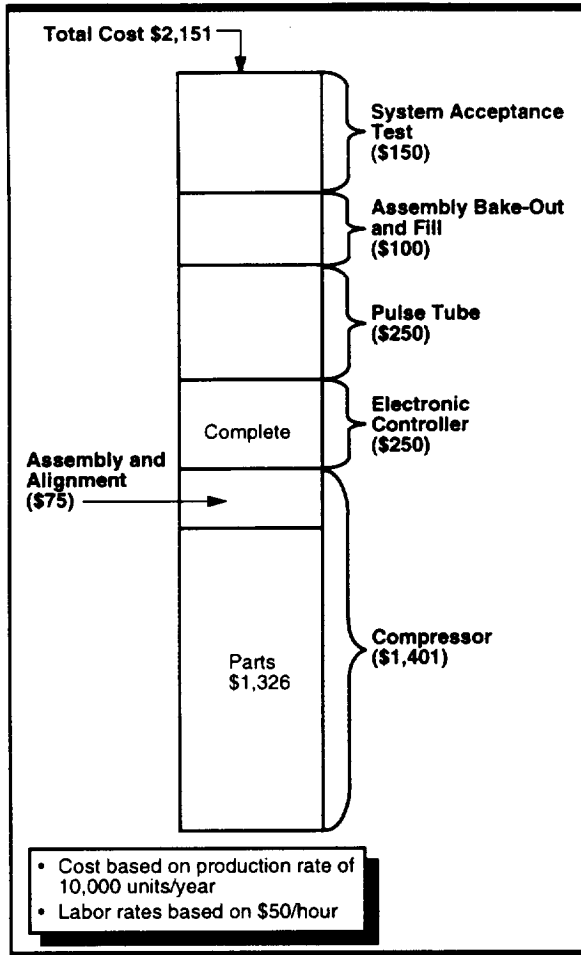
that can be adapted to computer control are also used. Computer control of the entire procedure will ultimately eliminate the need for skilled operators, resulting in improved repeatability and yields.

5.2 GAS BEARING COMPRESSOR

STI also conducted cost studies for their gas bearing compressor system. The results of these studies are summarized in Figure 5-3. These results are for the compressor only. The LM estimates of other costs summarized in Figure 5-4 may be added to these costs for a preliminary estimate of the total system costs.

Number of Units	50 Units (Present)	250 Units (Future)	2500 Units (Dedicated Assy Stations)
Total Piece Part & Processing Cost	\$1,352.93	\$1,184.48	\$567.52
Total Assy Labor	\$ 799.12	\$ 296.46	\$156.00
Total Costs	\$2,132.05	\$1,480.94	\$723.52

Figure 5-3. Compressor cost summary for STI gas bearing compressor system



LCC-020

Figure 5-4. Current commercial cryocooler cost estimate

5.3 SYSTEM COST STUDIES

The majority of the cost studies conducted on this program were focused on the compressor, since the parts cost was 65% of the project total system cost. Figure 5-4 summarizes the various costs for a flexure compressor system. The complete system cost is \$2,151 each in quantities of 10,000/year, including tooling and setup costs. The electronic controller system utilized feedback loops to control temperature and stroke, along with a high-efficiency pulse width modulator. Vendor quotes of \$250 each were received in 10,000/year quantities. Other labor costs were calculated at \$50/hour.

6.0 BUSINESS AND COMMERCIALIZATION PLANS

STI has prepared a business and commercialization plan to describe their products, customers and future plans. This plan is available separately because of its proprietary nature. Some of the information is covered in

Figures 6-1 through 6-7, which describes some of the primary features of this plan. Figure 6-7 describes a proposed program to continue the development through the insertion of the pulse tube technology into the STI products. This plan is under discussion at STI and LM.

<ul style="list-style-type: none"> • Customer Needs <ul style="list-style-type: none"> - Interference reduction - Expanded base-station coverage - Reduction of base-station size
<ul style="list-style-type: none"> • Market Size <ul style="list-style-type: none"> - HTS wireless receiver filters occupy 30% (\$570M) of the total wireless receiver filter market by 2002 (source: Northern Business Information)
<ul style="list-style-type: none"> • STI Products <ul style="list-style-type: none"> - Rack-mount and tower-mount platforms: 2-, 3-, and 6-channels - AMPS-A, AMPS-B, PCS, GSM frequency bands - With or without low-noise amplifier - Turn-key solution

Figure 6-1. Markets and Products—Commercial Wireless Market (cellular)

<ul style="list-style-type: none"> • Status <ul style="list-style-type: none"> - Shipped several units to several domestic and international cellular OEMs and service providers - Examples: <ul style="list-style-type: none"> -- Company A <ul style="list-style-type: none"> • Rack-mount passed accelerated life test • Placed field trial unit order: delivery in late 1997 -- Company B <ul style="list-style-type: none"> • Placed order for 8 HTS rack-mount and tower mount systems • One site currently up and running • Remaining system delivery scheduled through Q1'98 - Development of next generation platforms and filters in process - Sharper filters, high level of integration

Figure 6-2. Markets and Products—Commercial Wireless Market (cellular)

<ul style="list-style-type: none"> • Customer Needs <ul style="list-style-type: none"> - Low noise figure, high selectivity, high dynamic range - Broad or narrow-band operation - Frequency range from 10 MHz through 40 GHz - Tunable/switchable filters - Integrated, turn-key system
<ul style="list-style-type: none"> • Status <ul style="list-style-type: none"> - Shipped 2 turn-key HTS filter platforms - Developing 2 more cryocooled platforms

Figure 6-3. Markets and Products—Military Wireless

- | |
|--|
| <ul style="list-style-type: none"> • Current 4-Watt Stirling Cooler <ul style="list-style-type: none"> - Linear, integral stirling cycle, runs at 60 Hz - Free piston gas bearing - External coil - Lift of 4 Watts @ 77 K, @ 40°C heat-exchanger temperature - Designed for low cost and long life - Pilot production ramp-up effort currently underway - Life-testing and reliability improvement also underway |
| <ul style="list-style-type: none"> • Larger Cooler Development <ul style="list-style-type: none"> - Estimated lift of 6 Watts @ 77 K @ 40°C heat exchanger |

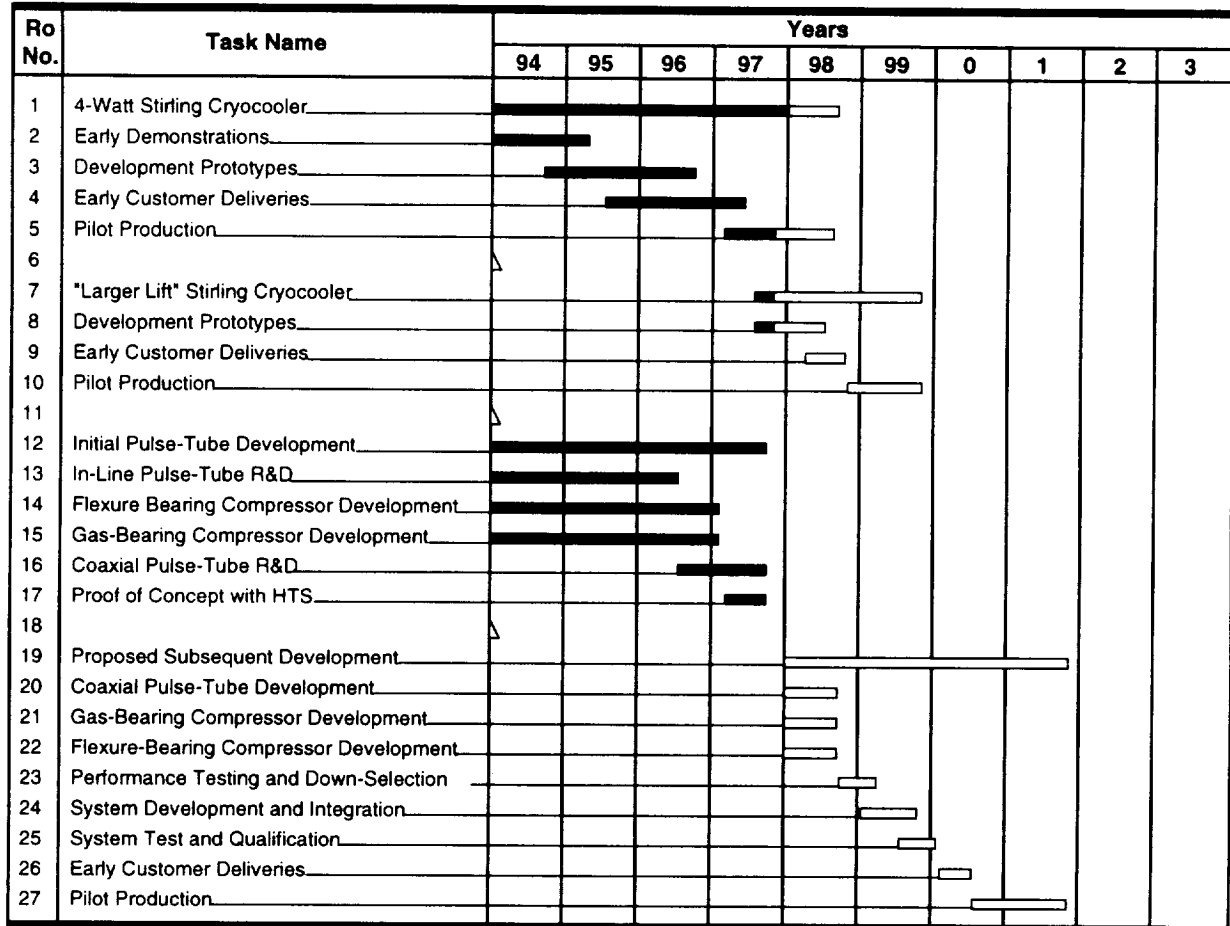
Figure 6-4. STI's Stirling Cooler Development Snapshot

- | |
|--|
| <ul style="list-style-type: none"> • Proof of Concept Successfully Completed <ul style="list-style-type: none"> - Coaxial pulse tube - HTS filter cooled |
| <ul style="list-style-type: none"> • Indications of Much Improved Performance (LM Mark III) <ul style="list-style-type: none"> - Higher lift, better efficiency |
| <ul style="list-style-type: none"> • Expectations of <ul style="list-style-type: none"> - Much longer life <ul style="list-style-type: none"> — One moving assembly, nothing moving in the cold end — Fewer critical alignment issues - More manufacturable, potentially lower cost |

Figure 6-5. STI's Interest in Pulse-Tube Technology

- | |
|---|
| <ul style="list-style-type: none"> • Develop Coaxial version of LM Mark III <ul style="list-style-type: none"> - Coaxial arrangement much more amendable to product integration |
| <ul style="list-style-type: none"> • Further Compressor Development <ul style="list-style-type: none"> - Gas bearing - Flexure bearing |
| <ul style="list-style-type: none"> • Performance Comparison and Down Selection <ul style="list-style-type: none"> - Compare the above two approaches with a series of tests typical of system operating environment, then choose the best solution |
| <ul style="list-style-type: none"> • System Development, Integration, Test, and Qualification <ul style="list-style-type: none"> - Platform development with pulse-tube cooler |
| <ul style="list-style-type: none"> • Incorporate into Product |

Figure 6-6. Required Program to Insert Pulse tube into Products



LCC-032

Figure 6-7. Proposed Cryocooler Development Program

7.0 NEW TECHNOLOGY

Several new technologies were developed in the process of designing the compressor for the low cost cryocooler. Major areas of inventions were:

1. Linear motor—a moving magnet and moving inner iron design
2. Flexure bearing alignment—self-centering diaphragm flexures in a one-piece housing
3. Piston/cylinder alignment—tilt adjustment mechanism
4. Position sensor—hall effect sensor between motor magnets

7.1 LINEAR MOTOR

The traditional approach to linear motors in cryocooler compressors employs a moving coil. The coil moves through a magnetic field generated by a stationary magnet/pole assembly. Flexing leads bring the required current to the coil to induce motion. The whole motor is generally located within the working fluid of the cooler.

The motor developed for this program reverses this arrangement and employs a moving magnet. The coil is stationary and is located outside the housing. This eliminates flexing leads and contamination of the working fluid with the epoxies used in the coil-winding process. In addition, there are no electrical connections required through the pressure wall. Unique to this motor is the moving inner pole piece which is attached to the moving magnet. This eliminates the moving magnetic field in this pole and the associated eddy current losses.

7.2 FLEXURE BEARING ALIGNMENT

Key to the assembly and operation of clearance-seal compressors is the very close fit of the moving piston within the stationary cylinder. Aligning the bearing system to produce the true linear motion required for this fit can be a time-consuming and tedious process.

The diaphragm flexures developed for this compressor, combined with the single-piece housing, are self-aligning at assembly and eliminate the need for adjustment. Integrated into these flexures are three small beams which act as contact points and flex to produce a controlled interference fit with the piston shaft. Similar beams interact with the housing bores. The result is that the flexures center themselves when pushed into the housing (which has precision bores at each end), and the piston centers itself when engaged in the flexures. The contact beams are produced by the same chemical milling process that produces the spiral flexures, and thus does not add to the overall cost of the parts.

7.3 PISTON/CYLINDER ALIGNMENT

Once the bearing system is running true, then it is possible to align the close-fitting cylinder to the piston to achieve the clearance seal. Experience has shown that it is harder to eliminate tilt between the cylinder and piston than it is to adjust for concentricity. Achieving proper tilt using shims and trial and error methods takes skilled technicians and is time consuming.

Developed specifically for this low cost compressor is an integrated, screw-operated, tilt adjustment mechanism. The adjusting screws are built into the cylinder support and act to flex the three bridges that hold the cylinder mounting pads. The bridges are formed by slots cut into the walls of the support and do not add to the overall parts count. Being able to continuously and precisely adjust tilt during the alignment process allowed the formation of a step-by-step procedure (using a special alignment fixture which optically tracks the position of the cylinder and displays it graphically in real time) which results in quick and reliable alignment.

The special alignment fixture is fitted with micro-positioners and force transducer feedback so that it could eventually be coupled to a computer for automated alignment.

7.4 POSITION SENSOR

The position sensors used to track the position of the piston and provide feedback to the electronic controller have traditionally required precise and expensive parts within the working fluid and electrical feedthroughs in the pressure wall.

To eliminate these problems, this compressor uses a low-cost commercial Hall effect-type sensor which picks up the magnetic field emanating from the moving magnets of the linear motor. The sensor can be mounted externally on the non-magnetic motor housing, but within the magnetic fields of the motor. The position of the piston can then be measured by the changing magnetic fields at the sensor.

8.0 ADVANCED DERIVATIVES UNDERWAY FROM THIS TECHNOLOGY

We have several new programs that are being funded from the technology developed under this program. These programs attest to the success of this technology, and are to a large extent driven by the reduced cost advantages of the approach developed. In these contracts we are basically utilizing the pulse tube-flexure compressor approach to develop higher capacity systems (up to 20 W at 77 K) and lower capacity miniature systems for cooling of 0.5 W at 80 K. In addition we are currently discussing a follow on program with STI to produce three prototype units based on our most recent pulse tube technology with both the flexure bearing compressor and the gas bearing compressor. A brief summary of these programs is given below.

8.1 DARPA PROGRAM FOR HIGH TEMPERATURE SATELLITE COMMUNICATION SYSTEMS

In this TRP program we are developing pulse tube cryocooler systems based on the flexure bearing/pulse tube system for higher (10 W) and lower (0.5-1.0 W) space based systems for

cooling to 77 K. These programs utilize our "Mark III" pulse tube technology.

High Cooling Capacity System

Figure 8-1 shows the utilization of two of the low cost flexure bearing compressors combined into a head to head configuration and feeding the pressure pulse to a pulse tube system. The load line of this system is presented in *Figure 8-2*, along with the power inputs in *Figure 8-3*. The applicability of this system to space operation has been investigated and we feel there is complete compatibility of the developed technology for space operation. Improvements in 3 areas of the system were evaluated for spaceborne operation: (1) Vibration balancing, achieved by tuned head to head compressor operation in such a way that the momentum of the two moving pistons is cancelled; (2) Improved motor efficiency, achieved in part by the head to head arrangement, which reduces the linear motor I²R losses and the identification of a more efficient, lower cost magnetic circuit arrangement; and (3) Enhanced ability to dissipate the waste heat in the vacuum environment of space, achieved by appropriate modified thermal conduction paths in the compressor.



LCC-030

Figure 8-1. Utilization of head to head compressors for a low pulse tube

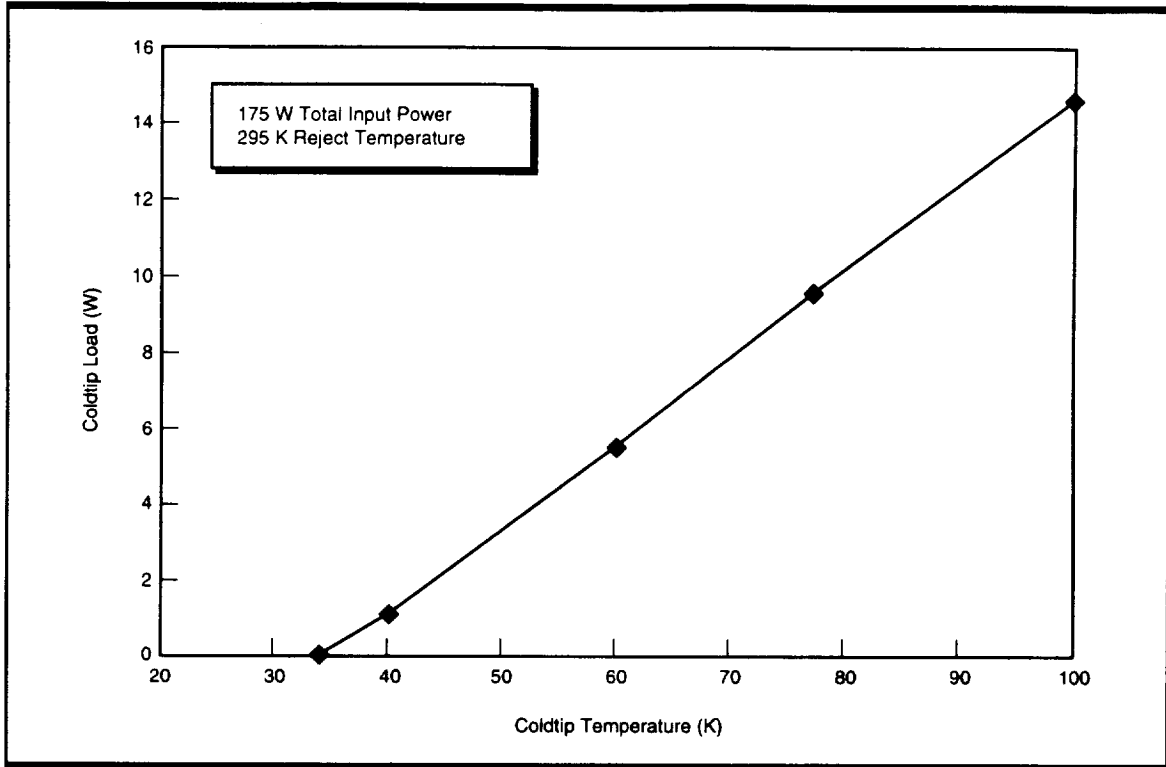


Figure 8-2. Load line of pulse tube with head to head low cost compressors

LCC-015

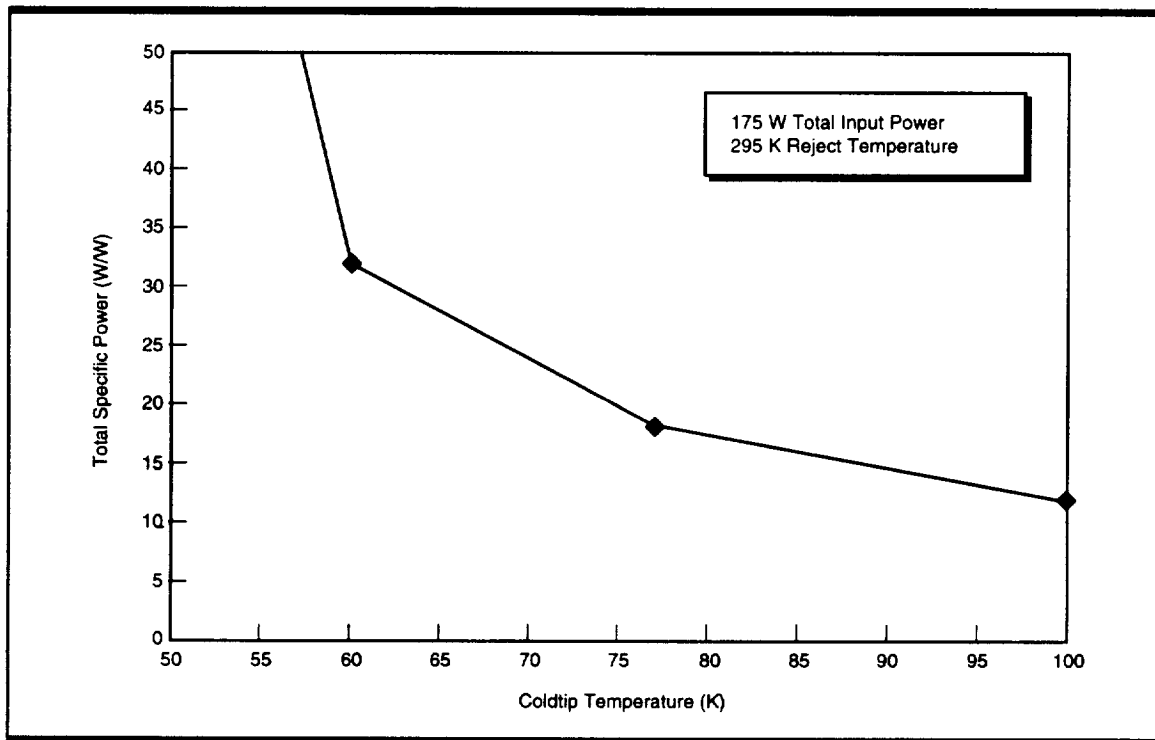


Figure 8-3. Specific compressor power for pulse tube with head to head low cost compressors

LCC-016

Low Capacity System

In this program we are developing pulse tube cryocoolers to provide 0.5 - 1.0 W at 77 K for low power input MUX elements of a high temperature superconductor spacecraft communication systems. The requirements of this part of the program are similar to the requirement for the NASA program below.

8.2 NASA/GSFC MINIATURE PULSE TUBE CRYOCOOLER

In this contract from NASA/GSFC we are utilizing the same basic technology approach to build a miniature pulse tube cryocooler with

weight of 1.25 Kg. This is a space based system with low cost potential. We have demonstrated the operation of the pulse tube system in the small size with a simulated compressor (a compressor with appropriate parameters to supply the same thermodynamic conditions to the pulse tube, as the final miniature compressor). The load line for this system is shown in *Figure 8-4*.

This program demonstrates the scaling to small sizes that can be achieved with this low cost technology.

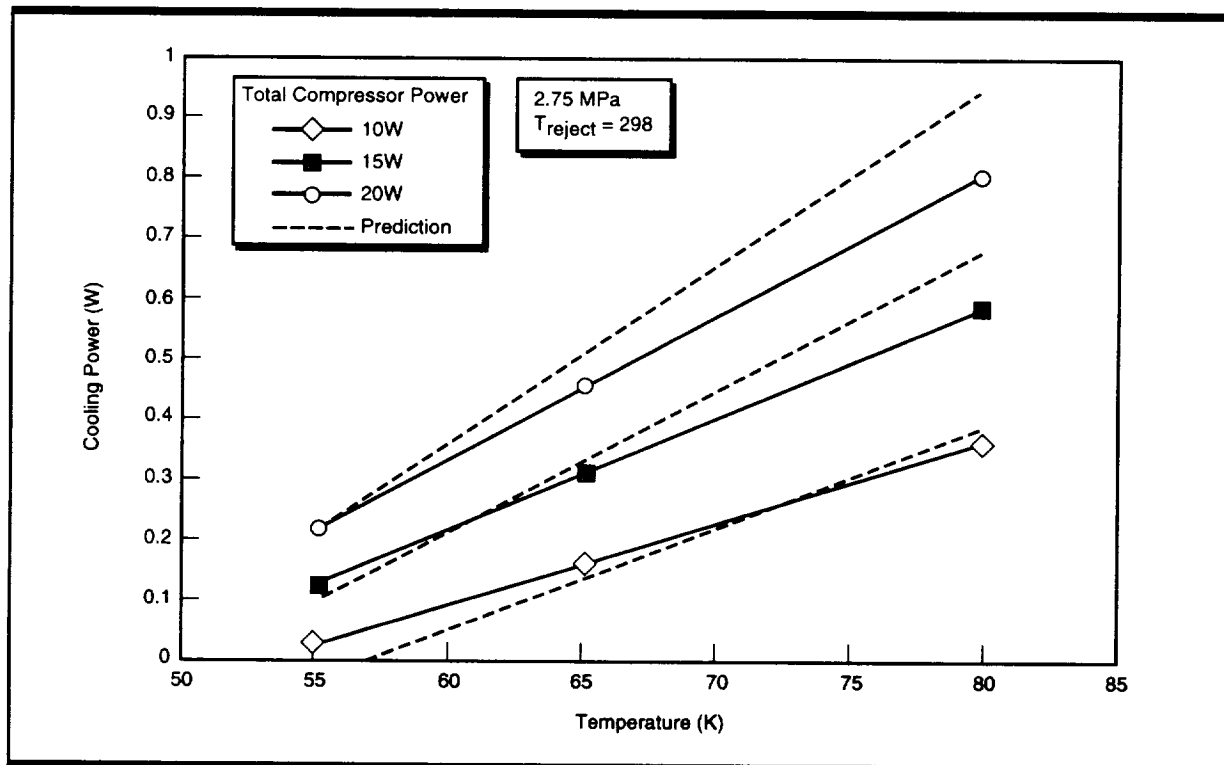


Figure 8-4. 45 Hz coldhead performance

LCC-017

9.0 SUMMARY AND CONCLUSIONS

The technology developed from this program was highly successful and met most of the goals of this program. A flexure bearing coaxial pulse tube system was integrated and tested with an STI dewar containing HTS filters. The results were completely successful showing the viability of the pulse tube technology with this system. Since this demonstration LM has substantially enhanced their pulse tube technology and with the same compressor and power input can now increase the cooling at 77 K from 3 W (demonstrated during the program) to 10 W with the same input power (170 W).

These systems have unlimited lifetime and have been shown to be low cost. The cost studies that have been conducted have estimated the total system cost to be \$2,151 each in production rates of 10,000 units per year for the flexure bearing compressor approach. The utilization of the pulse tube substantially reduces cost and improves reliability.

Two configurations of the pulse tube were developed; the so called in-line and the co-axial. We believe the in-line is somewhat more power efficient than the co-axial, but more definitive tests will be required to precisely quantify this difference. It appears to be no more than 10% and possibly less. The co-axial design approach was utilized for the integration and demonstra-

tion test with the STI filter dewar and offers major benefits in integration. This configuration permits a direct substitution of the pulse tube system for the Stirling presently in use at STI, therefore greatly easing the transition to the pulse tube system in STI products.

Substantial contributions to pulse tube technology were made in the program. Of particular value is the identification of a loss term in the thermodynamics which is designated as DC flow. Work from this program led to the 1st published account of DC flows (David Gedeon, 1996). The positive identification and demonstration of control and elimination of this effect was first reported based on work performed under this program. Exploration of a radical new type of regenerator was performed under this program. This "etched foil" regenerator was tested but complex fabrication issues led to poor performance.

Several additional programs and contracts evolved from this program and are under development for both higher and lower capacity cryocooler systems for both space and commercial applications. LM and STI are presently evolving a program to implement the pulse tube technology into their commercial programs.

A summary of the major accomplishments of this program is provided in *Figure 9-1*.

• Developed 2.8 W @ 77 K with the pulse tube cryocooler
• Developed concentric configuration for pulse tube
• 1st published account of dc flows (Gedeon-1996 Cryocooler Conference)
• Developed techniques for diagnosing and canceling dc flows
• Explored etched foil regenerator technology—not mature yet
• Successfully integrated pulse tube with STI filter dewar, demonstrated filter performance
• Developed a new low cost approach for a flexure bearing compressor
• Production costs for high rate production (10,000/yr) estimated at \$2,151 for flexure bearing pulse tube cryocooler

Figure 9-1. Summary of major accomplishments of the NASA-AITP program